Published in final edited form as:
Genes Brain Behav. 2007 February ; 6(1): 77–96. doi:10.1111/j.1601-183X.2006.00235.x.

Biochemical, molecular and behavioral phenotypes of Rab3A mutations in the mouse

S. Yang[†], **M. Farias**[†], **D. Kapfhamer**[†,‡], **J. Tobias**[§], **G. Grant**[†,§], **T. Abel**[¶], and **M. Bućan**[*,†,§]

[†]Department of Genetics, University of Pennsylvania, Philadelphia, PA,

[§]Penn Center for Bioinformatics, University of Pennsylvania, Philadelphia, PA, USA

[¶]Department of Biology, University of Pennsylvania, Philadelphia, PA, USA

Abstract

Ras-associated binding (Rab) protein 3A is a neuronal guanosine triphosphate (GTP)-binding protein that binds synaptic vesicles and regulates synaptic transmission. A mouse mutant, *earlybird (Ebd)*, with a point mutation in the GTP-binding domain of Rab3A (D77G), exhibits anomalies in circadian behavior and homeostatic response to sleep loss. Here, we show that the D77G substitution in the *Ebd* allele causes reduced GTP and GDP binding, whereas GTPase activity remains intact, leading to reduced protein levels of both Rab3A and rabphilin3A. Expression profiling of the cortex and hippocampus of *Ebd* and *Rab3a*-deficient mice revealed subtle differences between wild-type and mutant mice. Although mice were backcrossed for three generations to a C57BL/6J background, the most robust changes at the transcriptional level between $Rab3a^{-/-}$ and $Rab3a^{+/+}$ mice were represented by genes from the 129/Sv-derived chromosomal region surrounding the *Rab3a* gene. These results showed that differences in genetic background have a stronger effect on gene expression than the mutations in the *Rab3a* gene. In behavioral tests, the *Ebd/Ebd* mice showed a more pronounced mutant phenotype than the null mice; *Ebd/Ebd* have reduced anxiety-like behavior in the elevated zero-maze test, reduced response to stress in the forced swim test and a deficit in cued fear conditioning (FC), whereas $Rab3a^{-/-}$ showed only a deficit in cued FC. Our data implicate Rab3A in learning and memory as well as in the regulation of emotion. A combination of forward and reverse genetics has provided multiple alleles of the *Rab3a* gene; our studies illustrate the power and complexities of the parallel analysis of these alleles at the biochemical, molecular and behavioral levels.

Keywords

Behavior; GTPase; microarray; mouse mutant; Rab3A

Ras-associated binding (Rab) protein 3A plays a regulatory role in neurotransmitter release and calcium-triggered synaptic vesicle exocytosis (Sudhof 2004; Takai *et al*. 1996; Takai *et al*. 2001; Zerial & McBride 2001). Rab3A is the key member of the functionally redundant Rab3 family of small G proteins named Rab3A, Rab3B, Rab3C and Rab3D (Schluter *et al*. 2002; Schluter *et al*. 2004) and is the most abundant among these paralogs in the brain (Geppert *et al*. 1994). Rab3A functions by shuffling between a vesicle-associated guanosine triphosphate (GTP)-bound state and vesicle-dissociated GDP-bound state under regulation

[*]Corresponding author: Department of Genetics, University of Pennsylvania School of Medicine, Philadelphia, PA 19104, USA. bucan@pobox.upenn.edu.
[‡]Current address: Ernest Gallo Clinic and Research Center, Emeryville, CA,

by Rab GDP dissociation inhibitor (Rab GDI) (Matsui *et al*. 1990; Sasaki *et al*. 1990; Ullrich *et al*. 1993), GTPase activating protein (Rab3 GAP) (Fukui *et al*. 1997; Nagano *et al*. 1998), GDP/GTP exchange protein (Rab3 GEP) (Wada *et al*. 1997) and guanine nucleotide exchange factors (Burton *et al*. 1994; Luo *et al*. 2001). Several Rab3A effectors have been identified, including rabphilin3A (Li *et al*. 1994; Shirataki *et al*. 1992; Shirataki *et al*. 1993) and RIM1α/2α (Wang & Sudhof 2003; Wang *et al*. 1997; Wang *et al*. 2000), which bind only to GTP-Rab3A but not to GDP-Rab3A.

Electrophysiological studies of mice with a targeted loss-of-function mutation in *Rab3a* revealed altered short-term plasticity in synapses of the hippocampal CA1 region. The loss of Rab3A affected the late step of calcium-triggered vesicle exocytosis following transportation and docking (Geppert *et al*. 1994; Geppert *et al*. 1997; Schluter *et al*. 2004). Rab3A is also required for hippocampal CA3 mossy fiber long-term potentiation (LTP) and normal long-term depression (LTD), two forms of synaptic plasticity (Geppert *et al*. 1997). *Rab3A* mutants exhibit impairments in protein kinase A-dependent forms of corticoamygdala LTP and latephase LTP at hippocampal CA3-CA1 synapses (Huang *et al*. 2005). These phenotypes may be partly mediated by the interaction of Rab3A with its effector protein RIM1a (Betz *et al*. 2001; Powell *et al*. 2004; Schoch *et al*. 2002).

Behavioral assessments of *Rab3a*-null mutant mice have revealed normal hippocampus-dependent learning and memory in contextual fear conditioning (FC) as well as in the Morris water-maze test (D'Adamo *et al*. 2004; Hensbroek *et al*. 2003; Powell *et al*. 2004), although D'Adamo *et al*. reported moderately impaired platform reversal learning in the water maze in reference memory and episodic-like memory tasks (D'Adamo *et al*. 2004). In addition, Hensbroek *et al*. found reduced exploratory behavior, whereas D'Adamo *et al*. reported increased exploratory behavior in *Rab3a* knockout mice (D'Adamo *et al*. 2004; Hensbroek *et al*. 2003). Lastly, D'Adamo *et al*. reported reduced anxiety-like behavior in the same mice (D'Adamo *et al*. 2004), which was not detected by Powell *et al*. (Powell *et al*. 2004)

In addition to the targeted loss-of-function allele of *Rab3a*, a second allele, *earlybird* (*Rab3a*^{Ebd}), was identified independently using a forward genetic approach (Kapfhamer *et al*. 2002). *Ebd/Ebd* mice carry a point mutation that causes the replacement of aspartic acid with glycine in Rab3A's GTP-binding pocket, a highly conserved domain in all GTPases. Behavioral assessment of multiple rest-activity parameters in the *Rab3a*$^{-/-}$ and *Ebd/Ebd* mice revealed shortened circadian period of activity and anomalies in sleep homeostasis (Kapfhamer *et al*. 2002).

As the first step toward understanding the mechanisms that underlie the behavioral anomalies in *Ebd* mice, we examined the biochemical properties of the mutant form of Rab3A (Rab3A^{D77G}). We also compared *Ebd* and *Rab3a*$^{-/-}$ alleles at the transcriptome level by microarray analysis and at the behavioral level through a battery of tests. Our results show that disrupted GTP and GDP binding to Rab3A in *Ebd* mice and loss-of-function of Rab3A in *Rab3a*$^{-/-}$ mice affect learning and memory as well as emotional regulation, without significant changes in overall gene expression.

Materials and methods

Animals

Knockout mice for *Rab3a* (C57BL/6J; 129Sv-*Rab3a*^{tm1Sud}; stock code 002443) were obtained from the Jackson Laboratory (Bar Harbor, ME, USA) and backcrossed for three generations (N4) to C57BL/6J (B6). *Rab3a*^{Ebd} mice were identified in an ENU-mutagenesis screen of C57BL/6J mice (Kapfhamer *et al*. 2002), and after a cross to C3H/HeJ (C3), mice

were backcrossed for three generations (N4) to C57BL/6J. Mutant and wild-type mice were maintained on a light/dark (12:12) cycle with lights on at 0700 h. Food and water were available ab *libitum* using standard mouse hus-bandry procedures. All animal experiments were carried out according to the National Institutes of Health guidelines for the use of animals and were approved by the University of Pennsylvania Institutional Animal Care and Use Committee. Wild-type, heterozygous and homozygous mutant mice were generated by intercrossing *Ebd*/+ and *Rab3a*$^{+/-}$ heterozygous mice. At time of weaning (3 weeks), tail biopsies were taken to extract genomic DNA for genotyping. For *Ebd* mice, genotyping was performed by allelic discrimination on ABI Prism 7900HT (Applied Biosystems, Foster City, CA, USA) using a custom-designed single nucleotide polymorphism (SNP) assay that has a probe flanking the point mutation [A/G]. Genotypes were called automatically or manually using SDS 2.2 software (Applied Biosystems). The knockout line was genotyped as previously described (Kapfhamer *et al*. 2002). To assess the 129/Sv (129) or C3H-derived portion of the chromosome surrounding the *Rab3a* locus, the following 12 microsatellite markers were used for genotyping: D8Mit190.1, D8Mit46, D8Mit128, D8Mit25, D8Mit29, D8Mit73, D8Mit178.1, D8Mit304, D8Mit104, D8Mit348, D8Mit45.1 and D8Mit84. Among them, D8Mit46, D8Mit128 and D8Mit25 showed no detectable polymorphism between C57BL/6J and 129/Sv strains.

Tissue collection, RNA extraction and cDNA generation

For the analysis of both the *Ebd* and *Rab3a*$^{-/-}$ alleles, wild-type and homozygous mutant mice were sacrificed at Zeitgeber time 9. Cerebral cortex and hippocampus were dissected, frozen on dry ice and then transferred to −80 °C. Total RNA was isolated using TRIzol reagent (Invitrogen Life Technologies, Carlsbad, CA, USA) followed by cleanup using RNeasy mini kit (Qiagen Inc., Valencia, CA, USA). For all of these RNA samples, 1–2 μg was reverse transcribed using a High Capacity cDNA Archive Kit (Applied Biosystems) according to the manufacturer's instructions.

Cloning and expression of wild-type and Ebd mutant Rab3A

The cDNAs from the cortex of wild-type and *Ebd* mutant mice were used as template to amplify *Rab3a* by AccuPrime Pfx SuperMix (Invitrogen Life Technologies) using forward primer 5′-AGAGAGGGTAAGATGGCTTCC-3′ and reverse primer 5′-AATAGGGTAGTCGGGGATGG-3′. The polymerase chain reaction (PCR) products were inserted into the pCR2.1 vector using a TA Cloning Kit (Invitrogen Life Technologies) following the manufacturer's instructions. The wild-type and *Ebd* Rab3A cDNAs were then subcloned in-frame into the pcDNA3.1/His C vector (Invitrogen Life Technologies). Positive clones were confirmed by sequencing. HEK 293 (human embryonic kidney epithelial cell line) cells (kindly provided by Dr Adam Crystal) were transfected by Lipofectamine 2000 (Invitrogen Life Technologies) with pcDNA3.1/His C constructs harboring his-tagged wild-type and *Ebd* mutant Rab3A. Stable cell lines were selected by culturing cells in the presence of 0.5 mg/ml of geneticin. Cells were lysed by BD Xtractor, and his-tagged protein was purified by BD TALON affinity resin (BD Biosciences, Palo Alto, CA, USA).

Western blot analysis

The mouse brain tissues and the cells were homogenized in CelLytic MT (Sigma, St. Louis, MO, USA) in the presence of 2% proteinase inhibitor cocktail P-8340 (Sigma). The homogenates were centrifuged at 10 000 *g* at 4 °C for 20 min. The supernatants were applied to sodium dodecyl sulphate–polyacrylamide gel electrophoresis (SDS–PAGE), and the protein was transferred to a polyvinylidene fluoride (PVDF) membrane (Immobilon-P, MiliPore, Bedford, MA, USA). The blot was blocked at room temperature for 1 h in 5% fat-free milk dissolved in Tris buffered saline supplemented with 0.05% Tween 20. The primary

antibodies used were anti-His antibody (Amersham Biosciences, Piscataway, NJ, USA), anti-Rab3A (clone 42.2, Synaptic Systems, Gottingen, Germany), antirabphilin3A (polyclonal rabbit antibody, Synaptic Systems), anti-β-tubulin (clone 3B11, Synaptic Systems), anti-Rab GDI and anti-Rab GAP p130 (kindly provided by Professor Yoshimi Takai). The secondary antibodies were horseradish peroxidase (HRP)-conjugated sheep anti-mouse immunoglobulin (Ig)G and HRP-conjugated monkey anti-rabbit IgG (Amersham Biosciences). The protein amount was quantified by using ImageJ (http://rsb.info.nih.gov/ij/) and normalized to β-tubulin.

Co-immunoprecipitation

Co-immunoprecipitation was carried out according to published procedure (Nagano *et al*. 2002) with modifications. Briefly, HEK 293 cells were transfected with His-tagged Rab3A (wild type or mutant) and Myc-tagged rabphilin3A (a kind gift from Professor Yoshimi Takai). Cells were lysed in lysis buffer containing 20 mM Tris–Cl, pH 7.5, 100 mM NaCl, 1% Triton X-100, 1 mM EDTA, 0.5 mM PMSF and 0.5% protease inhibitor cocktail (P-8340, Sigma). After clearing the lysates with control IgG, Rab3A or rabphilin3A was immunoprecipitated using anti-His-G (Invitrogen Life Technologies) or anti-Myc (9B11, Cell Signaling, Danvers, MA, USA) monoclonal antibodies and protein A agarose (Invitrogen Life Technologies). SDS–PAGE and Western blots were performed as described above. To detect the interaction between Rab3A and rabphilin3A, Rab GDI and Rab GAP, cortex dissected from *Ebd* and knockout and their wild-type littermates was homogenized in lysis buffer described above. Immunoprecipitation was carried out using anti-Rab3A and then immunoblotted using antirabphilin3A, anti-Rab GDI and anti-Rab GAP.

[α-^{32}P]GTP overlay

The GTP-binding activity was examined by [a-^{32}P]GTP overlay assay according to Klinz *et al*. (Klinz 1994). Wild-type and *Ebd* mutant Rab3A proteins were resolved on SDS–PAGE without preheating and then immunoblotted onto a PVDF membrane (Immobilon-P, MiliPore). The membrane was incubated at room temperature for 1 h in binding buffer (50 mM Tris–Cl, pH 7.5, 20 μM $MgCl_2$, 1 mM DTT, 0.2% Tween-20) containing 1 μCi/ml of [α-^{32}P]GTP (Amersham Biosciences) and then washed six times for 10 min each with wash buffer (50 mM Tris–Cl, pH 7.5, 25 mM $MgCl_2$, 1mM DTT, 0.2% Tween-20). The blot was air-dried and exposed to X-ray film at −80 °C for 12–24 h.

[γ-35S]GTP and [^{3}H]GDP binding assays

The binding assays were carried out according to Giovedi *et al*. (Giovedi *et al*. 2004). Briefly, samples (1 pmol/25 μl) were incubated in binding buffer (20 mM Tris–Cl, pH 7.5, 10 mM EDTA, 5 mM $MgCl_2$,1 mM DTT) containing 0, 1, 3, 10, 30, 100, 300 and 1000 nM [γ-^{35}S]GTP or [^{3}H]GDP (PerkinElmer Life Sciences, Boston, MA, USA) for 30 min at 30 °C. Non-specific binding was determined in the presence of 300 μM GTP and GDP. The reaction was stopped by adding 1 ml of ice-cold stopping solution (25 mM Tris–Cl, pH 7.5, 20 mM $MgCl_2$, 100 mM NaCl), followed by rapid filtration on 0.45-μm nitrocellulose filters (Whatman, Maidstone, England). The radioactivity retained on the filters was determined by scintillation counting.

The [^{3}H]GDP dissociation assay

The assay was carried out as described (Giovedi *et al*. 2004; Kikuchi *et al*. 1995) with modification. Briefly, samples (2 pmol/24 μl) were incubated in loading buffer (20 mM Tris–Cl, pH 7.5, 10 mM EDTA, 5 mM $MgCl_2$, 1 mM DTT, 1 μM [^{3}H]GDP) at 30 °C for 20 min. Then 1 μl of 375 mM $MgCl_2$ was added, and samples were put on ice to stabilize the complex. The dissociation reaction was started by adding 75 μl of dissociation solution (20

mM Tris–Cl, pH 7.5, 200 mM NaCl, 2 mM $MgCl_2$,1 mM DTT, 67 μM GTP) and incubating at 30 °C for 0, 15, 30, 60 or 120 min. The dissociation reaction was stopped by filtration on 0.45-μm nitrocellulose filters, which were then subjected to scintillation counting.

GTPase assays

We employed two GTPase assays. The first (charcoal method) was carried out as described (Kikuchi *et al*. 1995). Wild-type and mutant Rab3A (25 pmol in 24-μl reaction) were loaded with [α-^{32}P]GTP by incubating proteins at 30 °C for 10 min in a loading buffer containing 20 mM Tris–Cl, pH 7.5, 100 mM NaCl, 1 mM EDTA, 1 mM DTT and 10 nM [α-^{32}P]GTP. The reaction was started by adding 1 μl of $MgCl_2$ to a final concentration of 5 mM. The reaction was stopped by adding 750 μl of ice-cold stopping solution (50 mM NaH_2PO_4,5% charcoal) at various time-points. Samples were centrifuged twice at 10 000 *g* at room temperature. The amount of [^{32}P] released from [α-^{32}P]GTP was determined by applying 400 μl of supernatant to scintillation counting. The second GTPase assay [thin layer chromatography (TLC) method] was performed as described (Giovedi *et al*. 2004) with modifications. Proteins (20 pmol in 20-μl reaction) were loaded with [α-^{32}P]GTP in loading buffer containing 10 nM [α-^{32}P]GTP. The reaction was started by bringing $MgCl_2$ to 5 mM. At indicated time, the reaction was stopped by adding 5 × stopping solution (1% SDS, 10 mM DTT, 10 mM EDTA, 2.5 mM GTP and 2.5 mM GDP) followed by incubating at 65 °C for 20 min. Samples were spotted to PEI-cellulose TLC sheets (Sigma) and air-dried for 20 min at room temperature. The TLC sheets were developed with 4M formic acid (pH 3.5 by NH_4OH). Then the sheets were air-dried and exposed to X-ray film at −80 °C. The amount of GTP and GDP was quantified using NIH ImageJ (http://rsb.info.nih.gov/ij/).

Microarray analysis

Arrays—We used Affymetrix expression set MOE430A/B (Affymetrix, Santa Clara, CA, USA), which consists of 45 037 probe sets representing 39 015 transcripts for 34323 genes. All protocols were conducted as described in the Affymetrix GeneChip Expression Analysis Technical Manual. Briefly, total RNA was isolated from the cortex and hippocampus of individual animals from *Ebd* line (+/+ and *Ebd/Ebd*, $n = 3$ each) and the knockout line (*Rab3a*$^{+/+}$ and *Rab3a*$^{-/-}$, $n = 6$ each). Five microgram of total RNA was converted to first-strand cDNA using Superscript II reverse transcriptase primed by a poly(T) oligomer that incorporated the T7 promoter. Second-strand cDNA synthesis was followed by *in vitro* transcription for linear amplification of each transcript and incorporation of biotinylated CTP and UTP. The cRNA products were fragmented to 200 nucleotides or less, heated at 99 °C for 5 min and hybridized for 16 h at 45 °C to MOE430A/B microarrays. The microarrays were then washed with low (6× SSPE) and high (100 mM MES, 0.1M NaCl) stringency buffers and stained with streptavidin-phycoerythrin. Fluorescence was amplified by adding biotinylated anti-streptavidin and an additional aliquot of streptavidin-phycoerythrin stain. A confocal scanner was used to collect fluorescence signal at 3 μm resolution after excitation at 570 nm. The average signal from two sequential scans was calculated for each microarray feature. Affymetrix Microarray Suite 5.0 was used to quantitate expression levels for targeted genes; default values provided by Affymetrix were applied to all analysis parameters. Border pixels were removed, and the average intensity of pixels within the 75th percentile was computed for each probe. The average of the lowest 2% of probe intensities occurring in each of 16 microarray sectors was set as background and subtracted from all features in that sector. Probe pairs were scored positive or negative for detection of the targeted sequence by comparing signals from the perfect match and mismatch probe features. The number of probe pairs meeting the default discrimination threshold (tau = 0.015) was used to assign a call (or flag) of absent, present or marginal for each assayed gene, and a *P* value was calculated to reflect confidence in the detection call. A weighted mean of probe fluorescence (corrected for non-specific signal by subtracting the mismatch

probe value) was calculated using the One-step Tukey's Biweight Estimate. This signal value, a relative measure of the expression level, was computed for each assayed gene. Global scaling was applied to allow comparison of gene signals across multiple microarrays: after exclusion of the highest and lowest 2%, the average feature signal was calculated and used to determine what scaling factor was required to adjust the chip average to an arbitrary target of 150. All signal values from one microarray were then multiplied by the appropriate scaling factor. The data files from MAS 5.0 were imported to GeneSpring 7 (Silicon Genetics, Redwood City, CA, USA) for further analysis. To minimize multiple testing problems in statistical analysis, the gene list was reduced by discarding those scored as 'absent' in two or more replicate samples. This resulted in 20 975 genes that were subjected to significance analysis of microarray (for information see http://www-stat.stanford.edu/~tibs/SAM/) and PaGE (Grant *et al*. 2005) to generate lists of statistically significant genes. The genes that showed a fold change more than 1.5 were considered as differentially expressed genes.

Real-time quantitative PCR and RT-PCR

Real-time PCR was carried out on ABI Prism 7900HT sequence detection system (Applied Biosystems) by relative quantification (ΔΔCt method) using GAPDH or 18S rRNA as the endogenous control. The template cDNAs were generated as described above and pooled from seven to nine animals per genotype. For each cDNA sample, we performed three or four technical repeats on the 384-well plates. The primer and TaqMan probe sets for target genes were either bought as Assays-on-Demand or ordered as Assays-by-Design by using the Assays-by-design File Builder (Applied Biosystems). The information for these assays (assay IDs and consensus sequences) is available upon request. Data files containing the Ct values from Applied Biosystems SDS 2.2 software were analyzed according to User Bulletin #2 for ABI Prism 7700 Sequence Detection System (Applied Biosystems). Reaction time (RT)-PCR was used to investigate the mRNA isoforms of Peroxiredoxin II (*Prdx2*) gene. The cDNAs were generated as described above, and PCR was done with Taq DNA polymerase (Roche, Indianapolis, IN, USA). To detect the longer (Prdx2-L) and shorter (Prdx2-S) isoforms, a common left primer was used: 5′-AGGACTTCCGAAAGCTAGGC-3′. The right primers for Prdx2-L and Prdx2-S are 5′-TGGATCTGGCGTTAAAGAGG-3′ and 5′-TTGACTGTGATCTGGCGAAG-3′, respectively. The PCR products were quantified by measuring the intensities of the bands using ImageJ (http://rsb.info.nih.gov/ij/).

Behavioral assessment

All behavioral testing was performed between 1400 and 1700 h with the experimenter blind to the subjects' genotype. A total of 7–23 male and female mice per genotype, aged 6–10 weeks, were used for behavioral assessment. The behavioral tests were performed in the following sequence: rotarod, zero maze, forced swim test (FST), Morris water maze, FC and acoustic startle/prepulse inhibition (PPI).

Rotarod—The test was performed according to published procedure (Tarantino *et al*. 2000). Mice were placed on the accelerating rotarod (Model 7650, Ugo Basile, Camerio VA, Italy), which accelerated at a constant rate from 4 to 40 rpm in 5 min, for a maximum time of 5 min. Mice were allowed to perform the test until they fell from the rod and given three trials with 45- to 60-min intertrial intervals. Rotarod performance reported here reflects the average performance of the second and third trials.

Zero maze—Behavior in the zero maze was assessed as previously reported (Tarantino *et al*. 2000). Mice were placed in one of the closed quadrants and were allowed to investigate the maze for 5 min in a single session. Mice were scored on several anxiety-related variables

as identified in previous studies including time spent in open quadrants and number of transitions between quadrants. The animals were tracked during the session by a Poly Track Video System (San Diego Instruments, San Diego, CA, USA) suspended approximately 130 cm above the maze.

FST—The FST is a validated model for studying the depressive-like behavior in rodents (Borsini & Meli 1988; Wieland & Lucki 1990). A single-day trial was used in which mice are individually placed in plexiglass cylinders (46 cm tall, 20.5 cm diameter) containing 23–25 °C water to a depth of 20 cm, for a total of 6 min. Mice were manually scored for total immobility time and time to first float (latency) during the entire 6-min trial, with 'immobility' defined as movement limited to that required to maintain the mouse's head above water. The water was changed between subjects. In a comparable forced swim set-up, C57BL/6J inbred mice showed sensitivity to different types of antidepressant drugs, including desipramine (Lucki *et al*. 2001).

Morris water maze—The Morris water maze can be used to assess spatial learning and memory in mice (D'Hooge & De Deyn 2001). Mice were placed into a 110-cm-diameter pool of opaque water (colored with white tempura non-toxic paint) at room temperature and trained over a 7-day period to locate a single hidden platform (area 10 cm^2) submerged 0.5 cm below the water surface. The maze was surrounded by several visual cues that remained constant in the room. Mice were subjected to four training trials per day, in which they were placed into each of four quadrants (NW, NE, SE and SW) and given a maximum 60 seconds to locate the platform, with an interval of 10 min between trials. Time to platform location (latency) was recorded for each trial. If a mouse failed to locate the platform, it was guided to the platform by the experimenter. Once on the platform, a 20-second acquisition period was provided before the mouse was removed from the maze and dried off. At the end of the training period, learning and memory was further assessed by a probe trial in which the platform was removed, and the path of the mouse through the maze was recorded using a video tracking system (San Diego Instruments). The recording was analyzed with Poly Track Video Tracking System software (San Diego Instruments), and the percent of total distance traveled and percent of total time spent in the platform quadrant were measured.

FC

The basic apparatus and procedure were as previously described (Lattal & Abel 2001). Mice were trained in a rectangular (16″L × 6″W × 8 3/8″H) FC chamber (Medical Associates; Columbus, OH, USA) for 120 seconds before the onset of a 30 seconds white noise tone [(conditioned stimulus (CS)]. At 148 seconds, a 1.5-mA foot shock [(unconditioned stimulus (US)] was administered through the floor of the apparatus for 2 seconds. The mice were removed from the chamber at 300 seconds. Mice were tested for contextual conditioning in the same chamber for 300 seconds, 24 h after training. For the cued conditioning test, the mouse was placed into a new chamber environment with the floor covered by a smooth, blue panel. Following 120 seconds in the altered context, the CS tone was administered for 180 seconds. 'Freezing' behavior was scored at intervals of 5 seconds during training (baseline freezing), immediately following cessation of the US (immediate freezing), during the 300 seconds in the same context (contextual conditioning), during the first 120 seconds of the cued trial (altered context freezing) and during the last 180 seconds of the cued trial (cued conditioning). Freezing was defined as complete lack of movement, except for respiration. Percent freezing was calculated as (no. of recorded freezes/no. of possible freezes) × 100.

Acoustic startle and PPI of acoustic startle

Acoustic startle response (ASR) and PPI of acoustic startle were measured using SR-Laboratory Systems (San Diego Instruments) according to published procedure (Tarantino *et*

al. 2000). After a 5-min acclimation period under continuous 70-dB white noise, mice were subjected to the following trials (×5) in pseudo-randomized order: 40-ms 90dB, 100dB, 110dB and 120dB, with average startle amplitude across the five 120-dB trials calculated as ASR. PPI was measured immediately after the Acoustic Startle test. The PPI session consisted of 15 trials spaced 15 s apart. Each trial consisted of a 40-ms 120dB stimulus delivered 60 ms after a 20 ms prepulse stimulus of either 70, 90 or 95dB. The ASRs for the 120 bB stimuli preceded by a 70dB prepulse were averaged and used to normalize the values obtained from the 90dB and 95dB prepulse trials. % PPI was calculated as: 100 - [(average ASR after 90 or 95dB prepulse/average ASR after 70bB prepulse) × 100]. % PPI values from the 90dB and 95dB prepulse trials were averaged to generate the final % PPI.

Statistical analysis

Statistical analysis was performed using either EXCEL software, or VASSARSTATS (http://faculty.vassar.edu/lowry/VassarStats.html). Strain effects among three genotypes were determined for most behavioral measures using a one-way analysis of variance (ANOVA), followed by Tukey post *hoc* tests when appropriate. The effects of genetic backgrounds and the interaction between mutations and backgrounds were examined by two-way ANOVA.

Results

Decreased GTP and GDP binding of Rab3A^{D77G} disrupts its interaction with effectors and causes reduced protein levels of Rab3A^{D77G} and Rabphilin3A

To compare *Rab3a*-null and *Ebd* mutants at the molecular and behavioral level, it was necessary to evaluate biochemical properties of the *Ebd* mutation. In the Rab3A protein, the *Ebd* mutation changes Asp^{77} in the highly conserved GTP-binding domain into Gly (Kapfhamer *et al*. 2002). On the basis of studies in other small GTPases (John *et al*. 1993; Jung *et al*. 1994; Ostermeier & Brunger 1999; Rak *et al*. 2003), we predicted that the *Ebd* mutation affects nucleotide binding. To test this prediction, we carried out biochemical assays for GTP/GDP binding, GDP dissociation and GTPase activity using wild-type and mutant Rab3A^{D77G} expressed in HEK293 cells. To examine the binding of GTP, two different assays were employed: an [α-^{32}P]GTP overlay assay and a [γ^{35}S]GTP binding assay. In the [α-^{32}P]GTP overlay assay, wild-type and Rab3A^{D77G} proteins were blotted to PVDF membranes that were examined for [α-^{32}P]GTP binding and protein amount. Wild-type Rab3A showed much stronger [α-^{32}P]GTP binding than Rab3A^{D77G}, indicating reduced GTP affinity for Rab3A^{D77G} (Fig. 1a). The [γ-^{35}S]GTP binding assay was carried out by employing a saturation binding experiment: wild-type and Rab3A^{D77G} proteins were incubated with various concentrations of [γ-^{35}S]GTP, and the proteinbound radioactivity was recovered by filtration through a nitrocellulose membrane and quantified by scintillation counting. Rab3A^{D77G} bound less [γ-^{35}S]GTP than wild-type Rab3A (Fig. 1b). This result, consistent with the result from the overlay assay, indicates that the *Ebd* mutation in Rab3A decreases GTP binding.

We next examined GDP binding in Rab3A^{D77G}. A saturation binding assay using [^{3}H]GDP as a radioligand showed that Rab3A^{D77G} bound less [^{3}H]GDP (Fig. 1c). In a [^{3}H]GDP dissociation assay, Rab3A^{D77G} showed faster GDP dissociation than wild-type Rab3A (Fig. 1d), providing independent evidence that GDP binding affinity is decreased in Rab3A^{D77G}.

To examine the intrinsic GTPase activity, we used TLC to measure the conversion of [α-^{32}P]GTP to [α-^{32}P]GDP by wildtype and mutant proteins. The amount of [α-^{32}P]GDP released from Rab3A^{D77G} was comparable to that from wild-type Rab3A (Fig. 1e). Similar results were obtained from a separate method measuring α-^{32}P release upon hydrolysis of

[α-^{32}P]GTP by wild-type and mutant Rab3A proteins (Fig. 1f). These results indicate that GTPase activity is not affected by the D77G mutation.

In addition to reduced GTP/GDP binding, *Ebd* mutant mice have reduced levels of Rab3A protein (Kapfhamer *et al*. 2002) (Fig. 2a). To address whether the decreased Rab3A protein in *Ebd* mice is due to decreased mRNA levels or changes in protein stability or degradation, we measured the mRNA level by real-time quantitative (Q) PCR using a probe that spans the exon 1–exon 2 junction so that it detects mutant and wild-type Rab3A mRNA equally well. In this assay, both wild-type and *Ebd* mice showed comparable Rab3A mRNA levels in brain tissues, whereas *Rab3a*$^{-/-}$ mice exhibited no detectable Rab3A mRNA (Fig. 2a). This result was further confirmed in independent samples by microarray analysis (see below). Therefore, we conclude that the point mutation in *Ebd* does not affect transcription of the *Rab3a* gene or the stability of Rab3A mRNA. Presuming that the point mutation is unlikely to affect the translation of Rab3A mRNA, the decreased Rab3A protein level in *Ebd* mice is most likely due to the decreased stability of the mutant Rab3A protein.

It was previously reported that rabphilin3A, a Rab3A effector, was decreased in *Rab3a*$^{-/-}$ mice (Li *et al*. 1994; Schluter *et al*. 2004). Our experiments confirmed this finding (Fig. 2b). Furthermore, we found that rabphilin3A protein was decreased by about 40% in the cortex and hippocampus of *Ebd* mice (Fig. 2b). Q-PCR and microarray analysis (data not shown) showed that the rabphilin3A mRNA level was not affected in the brain tissues of either *Rab3a* knockout or *Ebd* mice (Fig. 2b), indicating that the reduced rabphilin3A protein is due to decreased protein stability. The *Ebd* mutation and the loss of Rab3A do not lead to decreased protein levels of at least two other Rab3A effectors, Rab GDI and Rab GAP (Fig. 2c).

The interaction between Rab3A^{D77G} and its effectors, including rabphilin3A, Rab GDI and Rab GAP, was examined *in vivo* by co-immunoprecipition in cortex homogenates (Fig. 2d) and *in vitro* by co-immunoprecipition analysis in HEK293 cells co-transfected with Myc-tagged rabphilin3A and His-tagged wild-type or mutant Rab3A (Fig. 2e). Both sets of experiments showed that the *Ebd* mutation leads to decreased binding of Rab3A^{D77G} to rabphilin3A, Rab GDI and RabGAP. Furthermore, our experiment with the Rab3A^{D77G} protein shows that binding of rabphilin3A to Rab3A is required for the stability of rabphilin3A, as previously found in studies of Rab3A knockout mice (Li *et al*. 1994;Schluter *et al*. 2004).

Microarray experiments revealed subtle effects of Ebd and Rab3a-null mutations on gene expression in cortex and hippocampus

To compare the null and *Ebd* alleles at the molecular level and to investigate if they cause overall changes in gene expression, we performed transcription profiling by microarray analysis in two tissues (cortex and hippocampus) from four genotypes (+/+, Ebd/Ebd, Rab3a$^{+/+}$ and Rab3a$^{-/-}$).

Though Rab3A has wide-spread expression in central nervous system (Stettler *et al*. 1994), we used cortex and hippocampus as a tissue source for microarray analysis, because they can be easily dissected and samples can be collected from individual mice with no need for pooling. Furthermore, behavioral analysis of *Ebd* and *Rab3A*$^{-/-}$ mutants by us and others (D'Adamo *et al*. 2004; Hensbroek *et al*. 2003; Powell *et al*. 2004) revealed a wide range of behavioral anomalies in which the cortex and hippocampus play important roles.

The *Ebd* allele was generated on a C57BL/6J background and crossed for one generation to C3H/HeJ, whereas the *Rab3a*$^{-/-}$ allele was generated on a 129/Sv background and maintained on a mixed B6 × 129 background. To minimize the effect of genetic background

on molecular and behavioral phenotypes, we backcrossed both alleles for three generations to C57BL/6J. This three-generation backcross to C57BL/6J (N4 generation) would result in partial congenic lines consisting of approximately 94% C57BL/6J genome and approximately 6% C3H/HeJ in Ebd mice or 129/Sv in *Rab3a* knockout mice.

Global profiling of gene expression in Rab3A mutants and their wild-type littermates—There are three different parameters in the 36 samples of our microarray experiment. (a) Genotype at the *Rab3a* locus (*Ebd/Ebd* vs. +/+ and $Rab3a^{-/-}$ vs. $Rab3a^{+/+}$); (b) brain region (cortex vs. hippocampus) and (c) genetic background (B6.C3; N4 in *Ebd/Ebd* and +/+ mice vs. B6.129; N4 in $Rab3a^{-/-}$ and $Rab3a^{+/+}$ mice). We first asked how do these factors affect overall gene expression? To visualize overall similarities in expression patterns, we performed hierarchical clustering by Pearson Correlation of the genes that are present or marginal in at least two/three of the three or six replicates across all 36 samples. The condition tree indicates that the major factor that affects gene expression in our experiment is brain region specificity, because samples from the same brain region cluster together (Fig. 3a). Mice with different genetic backgrounds (B6.C3; N4 in *Ebd/Ebd* and +/+ mice vs. B6.129; N4 in $Rab3a^{-/-}$ and $Rab3a^{+/+}$ mice) have more dissimilar patterns of expression than mutant vs. wildtype (*Ebd/Ebd* vs. +/+ $Rab3a^{-/-}$ vs. $Rab3a^{+/+}$). This finding was confirmed by Principle Components Analysis on all 36 conditions (Fig. 3b–d). The first component captured 24% of the overall variability, the second component 10% and the third 6%. This result indicates that both mutations cause subtle changes in gene expression compared with brain region or genetic background of the mice.

The Ebd mutation of Rab3A has a subtle effect on gene expression—In *Ebd* alleles, no differentially expressed genes were identified with a false discovery rate (FDR) less than 10%. At a FDR around 50%, three genes in the cortex and two genes in the hippocampus were identified as having significantly altered expression (Table 1); however, their differential expression in *Ebd/Ebd* vs. +/+ was not confirmed by Q-PCR (data not shown). These genes may simply be false positives due to the high FDR (50%) in the microarray analysis, or they might have fallen beyond the resolution of Q-PCR due to the small fold change in their expression (mostly <twofold). Ultimately, the small number of genes identified as differentially expressed and the small fold changes of these genes indicate that the *Ebd* mutation has subtle, if any, effect on gene expression.

Differential gene expression in the $Rab3a^{-/-}$ mice due to congenic genomic sequence from 129/Sv background—In the $Rab3a^{-/-}$ mice, 23 genes including *Rab3a* were differentially expressed between $Rab3a^{-/-}$ and wild-type littermates in either the cortex or the hippocampus (Table 1). Among them, 18 map to the chromosomal region surrounding the *Rab3a* locus on mouse chromosome 8 (Fig. 4a). We examined the expression patterns of three differentially expressed genes (*Lpl, Slc5a5* and *Prdx2*) by Q-PCR or RT-PCR and confirmed the microarray results (see Supplementary material, Fig. S1). The expression patterns of these three genes in $Rab3a^{+/+}$ and $Rab3a^{-/-}$ strains were comparable to those in C57BL/6J and 129/Sv strains, respectively (see Supplementary material, Fig. S1). Furthermore, even the tissue-specific expression pattern of *Lpl* and the strain-specific splicing of *Prdx2* in $Rab3a^{-/-}$ corresponded to those detected in the 129/Sv strain (see Supplementary material, Fig. S2). Clustering of differentially expressed genes on chromosome 8 could be explained by differential gene expression between the 129/Sv chromosomal segment surrounding the genetically disrupted *Rab3a* gene and the C57Bl/6J wild-type chromosome. We thus genotyped the mice used for the microarray experiment at several chromosome 8 loci with a set of microsatellite markers which detect polymorphisms between the C57BL/6J and 129/Sv strains. In $Rab3a^{-/-}$ mice, the 129/Sv region shared by all mutant mice covers approximately 14 Mb (from 67 to 81 Mb, Ensembl m3.3) (Fig. 4b),

whereas all *Rab3a*$^{+/+}$ mice were homozygous for C57BL/6J at the region surrounding *Rab3a*. In *Ebd* mutant and wild-type mice, almost all tested chromosome 8 loci (10/12) were homozygous for C57BL/6J alleles (data not shown), indicating that remnants of the C3H/HeJ chromosome are dispersed across the genome in *Ebd* mutant and wild-type mice. This result indicates that the differentially expressed genes in the congenic region were regulated in a strain-specific manner. Therefore, we conclude that the *Rab3a*-null mutation *per* se has subtle effect on gene expression, as does the *Ebd* mutation.

Behavioral assessments revealed the role of Rab3A in learning and memory and in anxiety-related behavior

As a part of the overall characterization and comparison of the two *Rab3a* alleles, we examined behavior of mutant mice and their wild-type littermates in a battery of behavioral paradigms. These paradigms were selected with a goal of assessing several aspects of brain function, from motor abilities (rotarod), emotional behavior (zero maze), sensorimotor gating (PPI), stress-induced behavior (FST) to learning and memory (FC and Morris water maze).

Ebd and Rab3a-null mice exhibit intact spatial learning but impaired cued FC

—Spatial memory in *Ebd* and *Rab3a* knockout mice was assayed in a hidden platform version of the Morris water maze. This paradigm involves training mice for 7 days to locate a submerged platform, followed by a probe trial in which the platform is removed and the preference for the quadrant of the pool in which the platform was located is determined by measuring percent time spent and swim distance in the platform quadrant. Both *Ebd* and *Rab3a* knockout mice exhibited a rapid decline in latency as the training period progressed (Fig. 5a). In the *Ebd* line, no statistical difference was observed for either the percent total distance traveled in the platform quadrant ($F_{2,24}$ = 0.396, P = 0.677) or percent time spent in the platform quadrant ($F_{2,24}$ = 0.290, P = 0.751) during the probe trial. Similarly, *Rab3a* knockout mice showed no significant difference in percent distance ($F_{2,22}$ = 2.911, P = 0.078) and percent time ($F_{2,22}$ = 2.829, P = 0.083) spent in the platform quadrant during the probe trial. The results indicate that neither the *Ebd* nor the *Rab3a*$^{-/-}$ allele affects spatial learning and memory performance. Nonetheless, two-way ANOVA detected significant effect of genetic background between *Ebd* and *Rab3a* knockout lines in both percent distance ($F_{1,47}$ 9.71, P = = 0.003) and percent time ($F_{1,47}$ = 12.72, P = 0.0009) in the platform quadrant, although no interaction between background and genotypes was observed ($F_{2,47}$ = 1.79, P = 0.180 for percentage distance and $F_{2,47}$ = 1.84, P = 0.171 for percentage time). Our results support previous reports on differences between the 129/Sv and the C57BL/6J lines in the Morris water-maze test (Owen *et al*. 1997b).

The FC test is another measure of learning and memory in mice. This paradigm tests a mouse's ability to associate a mild foot shock (US) with a specific environment (contextual FC, environment CS) and a tone (cued FC, tone CS); memory of the US is signified by freezing behavior observed in the mouse. *Ebd* and *Rab3a* knockout mice were subjected to both FC tests and were compared in baseline (without US), immediate (following US), contextual (environment CS, no US), altered context (no US) and cued (tone CS, no US) freezing. Mice from both lines exhibited similar baseline and immediate freezing (data not shown). All mice performed similarly in the contextual FC [*Ebd* lines: $F_{2,36}$ = 0.23, P = 0.796; *Rab3a*$^{-/-}$ lines: $F_{2,24}$ = 0.265, P = 0.77; genetic backgrounds: $F_{1,61}$ = 3.54, P = 0.065], thus neither mutations of Rab3A nor genetic background affected this type of hippocampal-dependent learning (Fig. 5b). In contrast, both *Ebd/Ebd* mice ($F_{2,53}$ = 3.853, P < 0.05) and *Rab3a*$^{-/-}$ mice ($F_{2,32}$ = 8.943, P < 0.001) displayed impaired cued FC learning, as compared to their wildtype controls (Fig. 5b). This potentially implicates Rab3A in some aspect of amygala-dependant learning.

Ebd mice, but not Rab3a$^{-/-}$ mice, show reduced anxiety-like, decreased behavioral despair behavior as well as acoustic startle-induced hyperekplexia

—To further evaluate the observed anomalies in Rab3A mutant mice, we assessed other behavioral phenotypes in these mice. Neuromuscular coordination and strength in *Ebd* and *Rab3a*$^{-/-}$ mice were examined using an accelerating rotarod (Fig. 6a). No difference was observed among the three genotypes of *Ebd* lines (*Ebd/Ebd*, *Ebd*/+, and +/+) ($F_{2,25} = 0.533$, $P = 0.594$) and the three genotypes of *Rab3a*$^{-/-}$ lines (*Rab3a*$^{-/-}$, *Rab3a*$^{+/-}$ and *Rab3a*$^{+/+}$) ($F_{2,28} = 1.385$, $P = 0.268$). This result indicates that neither the loss-of-function nor the *Ebd* mutation affect neuromuscular coordination or motor ability and affirmed that the anomalies observed in other behavioral tests were not consequences of mutant Rab3A-induced neuromuscular dysfunction. However, two-way ANOVA did reveal an effect of genetic background between *Ebd* and *Rab3a*$^{-/-}$ lines ($F_{1,54} = 4.52$, $P = 0.039$).

We used the elevated zero maze to test anxiety-like behavior in *Ebd* and *Rab3a*$^{-/-}$ mice. The time that a mouse spends in the open areas and the number of transitions between open and closed quadrants are indicative of anxiety-like behavior, such that increased time in the open quadrants and increased transitions are predictive of low anxiety (Borsini & Meli 1988). The *Ebd/Ebd* and *Ebd*/+ mice showed an increased number of transitions ($F_{2,53} = 8.878$, $P < 0.001$) and spent longer time in open quadrants ($F_{2,53} = 15.613$, $P < 0.001$), indicating reduced anxiety-like behavior in these mice (Fig. 6b). Among the *Rab3a*$^{-/-}$ lines, no difference was observed in either the number of transitions ($F_{2,32} = 0.124$, $P = 0.884$) or the time spent in the open quadrants ($F_{2,32} = 0.903$, $P = 0.416$) (Fig. 6b). Two-way ANOVA revealed significant interaction between genetic background and genotypes in both transitions ($F_{2,86} = 4.08$, $P = 0.021$) and time in open quadrants ($F_{2,86} = 3.73$, $p = 0.028$), suggesting that the genetic backgrounds of *Ebd* and *Rab3a*$^{-/-}$ lines affect anxiety-like behavior differently.

Mice from the *Ebd* and *Rab3a*$^{-/-}$ lines were subjected to the FST to evaluate response to stress. In this test, increased float time or shorter latency (swim time before first float) is indicative of increased 'behavioral despair'. No difference in the latency before first float was observed in either the *Ebd* line ($F_{2,50} = 1.736$, $P = 0.187$) or the *Rab3a*$^{-/-}$ line ($F_{2,30} = 2.996$, $P = 0.066$) (Fig. 6c). The genetic background of the *Ebd* and *Rab3a*$^{-/-}$ lines have negligible effect on the latency in FST ($F_{1,81} = 0.76$, $P = 0.386$). In contrast, a significant strain effect of total float time was observed in the *Ebd* lines ($F_{2,50} = 3.592$, $P = 0.035$), with decreased total float time in *Ebd/Ebd* mice relative to wild-type controls ($P < 0.05$, Tukey HSD test) (Fig. 6c). *Rab3a*$^{-/-}$ mice, however, showed no difference in total float time ($F_{2,30} = 0.148$, $P = 0.863$). Genetic background had a significant effect on this behavior ($F_{1,81} = 38.53$, $P < 0.001$). These observations suggest that the *Ebd* mutation leads to decreased behavioral despair in the FST and that the different performance of *Ebd* and *Rab3a*$^{-/-}$ lines in this test is due to their different genetic backgrounds.

The startle test assesses sensorimotor processing (Koch & Schnitzler 1997), while PPI of the acoustic startle reflex (ASR) is a measure of sensorimotor gating in humans and rodents (for a review, see Swerdlow *et al*. 2001). The magnitude of the ASR was significantly increased in *Ebd/Ebd* and *Ebd*/+mice ($F_{2,64} = 5.482$, $P = 0.01$) compared to wild-type controls, although no difference was observed in *Rab3a*$^{-/-}$ lines ($F_{2,39} = 0.313$, $P = 0.734$) (Fig. 6d). Genetic background had a significant effect on acoustic startle ($F_{1,104} = 42.32$, $P < 0.001$) (Fig. 6d). For PPI, there were no differences within either *Ebd* lines ($F_{2,64} = 0.297$, $P = 0.74$) or *Rab3a*$^{-/-}$ = lines ($F_{2,39} = 0.622$, $P = 0.542$); however, genetic background affects PPI significantly ($F_{1,104} = 52.75$, $P < 0.001$), with the *Rab3a*$^{-/-}$ lines showing higher percentage PPI than the *Ebd* lines (Fig. 6d). This result suggests that the *Ebd* mutation affects sensorimotor processing without affecting sensorimotor gating and that differences

observed between *Ebd* and *Rab3a*$^{-/-}$ lines in this test are due to their different genetic backgrounds.

Discussion

Previous genetic studies of Rab3A, a small GTP-binding protein, focussed on studies of the null mutation in the mouse and its role in vesicle trafficking and neurotransmitter release (Geppert *et al*. 1994; Geppert *et al*. 1997; Schluter *et al*. 2004). We have described the identification of *Ebd*, an ENU-induced point mutation in the *Rab3a* gene, which results in the replacement of aspartate with glycine in the highly conserved GTP-binding domain of Rab3A (Kapfhamer *et al*. 2002). Here, we compare two Rab3A mutations, null and *Ebd*, at a molecular and biochemical level, with the goal of relating their effects to observed behavioral anomalies.

D77G mutation in Rab3A causes reduced binding of effectors and reduced stability of Rab3A and rabphilin3A proteins

Previous *in vitro* studies of Rab3A involved analysis of a series of mutations in rat Rab3A and a yeast ortholog Ypt1, including their effects on intrinsic GTPase activity, GDP dissociation rate and GDP or GTP binding (Becker *et al*. 1991; Brondyk *et al*. 1993; Burstein *et al*. 1992; Wagner *et al*. 1987). Mutations in the aspartic acid of the Asp-X-X-Gly (DXXG) motif common to all GTP-binding proteins have not been reported in any Rab3A ortholog. The crystal structures of the GppNp-bound Rab3A and Ypt1-GDI complexes implicate the role of D77 in Rab3A and D63 in Ypt1 in Mg^{2+} binding, which is important for nucleotide binding and hydrolysis (Ostermeier & Brunger 1999; Rak *et al*. 2003). Functional consequences are known for mutations in the corresponding amino acid in human H-Ras; H-RasD57Y shows higher affinity for GDP than for GTP (Jung *et al*. 1994), and H-RasD57A has increased GDP binding and reduced GTPase activity (John *et al*. 1993). However, replacement of the same aminoacid by asparagine (H-RasD57N) did not alter the biochemical properties of H-Ras (Farnsworth & Feig 1991). Our studies of mouse Rab3A showed that replacement of aspartic acid by glycine in Rab3A^{D77G} lowers the affinity for both GTP and GDP but leaves GTPase activity intact. On the basis of these findings, we postulate that under physiological conditions, the *Ebd* mutation shifts Rab3A away from its active form.

In the Rab3A-null mutant, the absence of Rab3A protein leads to a decreased level of rabphilin3A protein (Li *et al*. 1994). We have also observed reduced levels of rabphilin3A in *Ebd* mutants, and the reduction seems to be comparable to that caused by the null mutation. Co-immunoprecipitation revealed reduced binding between rabphilin3A and Rab3A^{D77G}, suggesting that the binding of rabphilin3A to functional Rab3A protein is required for its stability. This, in accord with previous studies of synapsin I and synapsin II (Rosahl *et al*. 1995), illustrates that in a presynaptic neuron, loss of specific protein–protein interactions can lead to protein instability and degradation. Though the absence of rabphilin3A does not affect neurotransmission in hippocampal neurons in mice (Schluter *et al*. 1999), rabphilin3A does potentiate SNARE function independently of Rab3A (Staunton *et al*. 2001). Furthermore, it has been shown that phosphorylated rabphilin3A is region-specifically distributed in rat brain, with the highest levels in the cerebellum, midbrain and medulla (Foletti & Scheller 2001). It is possible therefore that the reduction of rabphilin3A protein perturbs the function of a subset of synapses in some specific brain regions. Rab3A^{D77G} also has reduced binding affinity for Rab GDI and Rab GAP, though neither the *Ebd* nor the null mutations of Rab3A affected the protein levels of these Rab3A effectors. Rab GDI retrieves GDP bound form of Rab proteins from the membrane by forming a heterodimer that serves as a cytosolic reservoir for inactive Rabs (Sasaki *et al*. 1990). Systematic expression profiling indicates that Rab3A is the most abundantly expressed Rab family member in the

brain (Gurkan *et al*. 2005) and thus represents the major substrate for Rab GDI. The reduced affinity between Rab3A^{D77G} and Rab GDI may cause an increase of inactive Rab3A^{D77G} bound to the membrane, which may interfere with normal vesicle trafficking. It is important to note that mutations in *GDI1* have been implicated in X-linked non-specific mental retardation (D'Adamo *et al*. 1998), and *Gdi1*-deficient mice show altered associative memory and social behavior (D'Adamo *et al*. 2002). On the basis of the genetic evidence, we suggested that the *Ebd* mutation represents a dominant negative allele of *Rab3a* (Kapfhamer *et al*. 2002). Although our results describe biochemical changes in several Rab3A effectors caused by the D77G substitution; further studies are required to show which, among a large number of Rab3A interacting proteins, are responsible for the robust behavioral consequences of the mutation.

Mutations of Rab3A do not cause robust changes at the transcriptome level

Expression profiling of *Ebd* and *Rab3a*$^{-/-}$ mice and their wildtype littermates revealed subtle, if any, changes caused by the presence of the Rab3A mutations. Therefore, we conclude that disruption of Rab3A function, either by its absence or a mutation in the GTP-binding domain, leads to molecular changes and behavioral anomalies mainly through changes at the post-transcriptional level. For example, our microarray experiment, as well as Q-PCR, showed that the reduced level of rabphilin3A is not caused by a reduced level of mRNA but rather by the stability of rabphilin3A protein. We do not attribute the absence of global changes in gene expression in Rab3A mutants to technical problems or our inability to detect subtle changes in gene expression by microrrray technology because of the successful detection of 18 genes that are differentially expressed between the 129/Sv and C57BL/6J in the congenic line. We also considered that the lack of transcriptional changes may be explained by functional redundancy between the *Rab3a*, *Rab3b*, *Rab3c* and *Rab3d* genes; however, in our microarray experiment, we did not detect changes in the expression levels of these paralogs in *Rab3a*$^{-/-}$ or *Ebd* mice.

It is remarkable that the only robust changes in gene expression between mutant *Rab3a*$^{-/-}$ and wild-type mice can be attributed to differences in genetic background. Two mutant lines were originally generated on two different chromosomes, *Ebd* on C57BL/6J and *Rab3a*$^{-/-}$ on 129/Sv. Both lines were backcrossed to C57BL/6J for three generations; however, in the case of *Ebd*, the series of backcrosses followed an original outcross to C3H/HeJ. Therefore, during backcrossing and selection for a mutant *Rab3a*$^{-/-}$ locus, remnants of the 129/Sv (donor strain) were inherited as so-called passenger loci. In *Ebd* mice, differential chromosomal segments are scattered throughout the genome. On the basis of the calculations (Flaherty 1981; Silver 1995) as well as empirical data, we expected that a three-generation backcross of the *Rab3a*$^{-/-}$ line on a 129/Sv chromosome to a C57BL/6J background would leave a large segment (approximately 50 cM) of the donor chromosome (129/Sv) around the *Rab3a* locus that serves as a target in selection. Through genotyping of all lines used for microarray analysis, we showed that the differential chromosomal segment in *Rab3a*$^{-/-}$ covers > 14 Mb and contains 178 genes according to ENSEMBL (mouse m33 version). This high gene number supports reports that this segment of mouse chromosome 8, and the orthologous region on human chromosome 19, represents the most gene-dense region in the mammalian genome (Dehal *et al*. 2001). Furthermore, our finding that 18 among 178 genes show differential expression between 129/Sv and C5BL/6J chromosomes may be explained by an exceptionally high degree of nucleotide variation, including non-synonymous coding SNPs and stop codons, between these two genomes (Adams *et al*. 2005).

Rab3A is involved in learning and memory as well as in emotional regulation

In our original publication, we reported that *Ebd* and *Rab3a*$^{-/-}$ mice have shortened circadian period and decreased response to sleep loss (Kapfhamer *et al*. 2002). Mutants with sleep and circadian anomalies provide useful models for the analysis of a link between these neurobiological systems and mood disorders in humans. For example, *Clock* mice have sex-specific changes in exploratory and escape-seeking behavior, with no changes in anxiety and depression-like behavior (Easton *et al*. 2003). Moreover, studies of circadian mutants in Drosophila showed that the *period* gene plays a key role in long-term memory formation (Sakai *et al*. 2004). Therefore, we conducted a comparison of two alleles, *Ebd* and *Rab3a*$^{-/-}$, using a comprehensive battery of behavioral tests, including those for anxiety, sensorimotor gating, response to stress and learning and memory.

Electrophysiological experiments in *Rab3a* knockout mice established a role for Rab3A in hippocampal mossy fiber LTP and LTD (Castillo *et al*. 1997; Geppert *et al*. 1997), two forms of synaptic plasticity generally accepted as necessary for the consolidation of certain types of long-term memory. On the basis of these LTP/LTD phenotypes, one might predict that *Rab3a* mutant mice would exhibit altered performance in hippocampal-dependent learning paradigms. However, both contextual FC and performance in the Morris water maze were normal in *Ebd* and *Rab3a* knockout mice, indicating that hippocampal-dependent learning/memory does not require Rab3A. Both contextual and cued FC depend on the amygdala, whereas contextual FC also involves the hippocampal system, depending on the exact nature of the FC protocol followed (Kim & Fanselow 1992; Matus-Amat *et al*. 2004; Phillips & LeDoux 1992). The observed deficit in cued FC in both *Ebd/Ebd* and *Rab3a*$^{-/-}$ mice suggests that alterations in Rab3A-meditated neurotransmission may underlie this deficit and provides evidence for a role of Rab3A in memory processes outside the hippocampus. Our results to some extent support a role for Rab3A in LTP in the cortical pathway to the amygdala as observed by Huang *et al*. (Huang *et al*. 2005), but how this explains the selective deficits in cued but not contextual conditioning remains unclear. Other studies failed to detect an effect on cued FC in the *Rab3a* knockout line (D'Adamo *et al*. 2004; Hensbroek *et al*. 2003; Powell *et al*. 2004), probably due to differences in genetic background of the mice used in the studies, differences in age of tested mice and/or experimental environments (see below). Although one may question the validity of our findings for the *Rab3a* knockout mice due to differential expression of >18 genes in the 129/Sv chromosomal segment surrounding the *Rab3a* gene, anomalies in cued FC detected in the *Ebd* allele are more likely to be due to the disruption of the *Rab3a* gene because in *Ebd* mutants a small contributions from the C3H-derived genome (6%) is randomly distributed in both mutant and wild-type progeny. It is interesting that our studies reveal impairments in cued FC but not in contextual conditioning. This suggests that different neuronal circuits (perhaps within the amygdala) may mediate these distinct forms of FC, an idea that is supported by several other studies in which a similar phenotype of impaired cued FC but normal contextual conditioning was observed (Barnes & Good 2005; Gould & Feiro 2005) as well as the finding of distinct QTLs for cued and contextual conditioning (Owen *et al*. 1997a).

In contrast to the *Rab3a* knockout line, *Ebd* mice exhibited altered performance in the zero maze, forced swim and startle tests, which may be due either to a dominant-negative effect of the *Ebd* mutation or a background effect that masks the phenotypes in *Rab3a* knockout mice. The reduced anxiety-like behavior is consistent with impaired performance in cued FC, given the fact that both fear and anxiety involve the amygdala (Charney & Deutch 1996; Davis 1998) and the same mesolimbic dopaminergic pathways (Pezze & Feldon 2004). However, the enhanced acoustic startle response seems to be inconsistent with decreased anxiety in *Ebd* mice, because anxiety enhances the acoustic startle response in both rodents and humans (Koch 1999). A possible resolution lies in the fact that the neuronal circuits

mediating acoustic startle response and anxiety are different. The acoustic startle response circuit is located in the lower brainstem with the caudal pontine reticular nucleus playing a key role in the primary acoustic startle response pathway, and both excitatory transmitter glutamate and inhibitory GABA are involved (Koch 1999). Anxiety, by contrast, is regulated by the limbic-hypothalamic-pituitary-adrenal axis (Lopez *et al*. 1999), and a pivotal role for the amygdala was suggested in the transmission and interpretation of fear and anxiety (Charney & Deutch 1996).

Although the main purpose of behavioral studies reported in this paper is to compare anomalies in two *Rab3a* alleles, *Ebd* and *Rab3a*$^{-/-}$, we can compare or calibrate our findings to several previously reported behavioral studies of *Rab3a*$^{-/-}$ mice (D'Adamo *et al*. 2004; Hensbroek *et al*. 2003; Powell *et al*. 2004). The most consistent finding observed by all four studies is normal hippocampus-dependent learning and memory in contextual FC assay (D'Adamo *et al*. 2004; Hensbroek *et al*. 2003; Powell *et al*. 2004). Moreover, all reports are consistent with normal spatial learning performance of *Rab3a*$^{-/-}$ mutants in the conventional form of the Morris water maze (D'Adamo *et al*. 2004; Hensbroek *et al*. 2003; Powell *et al*. 2004), although D'Adamo *et al*. (D'Adamo *et al*. 2004) reported moderately impaired platform reversal learning in the water maze in reference memory and episodic-like memory tasks. Hensbroek *et al*. found reduced exploratory behavior in *Rab3a* knockout mice, while D'Adamo *et al*. reported the opposite result (D'Adamo *et al*. 2004; Hensbroek *et al*. 2003), and we detected no anomalies in exploratory behavior tested in the hole board (data not shown). We and D'Adamo *et al*. report reduced anxiety-like behavior, which was not detected by Powell *et al*. (D'Adamo *et al*. 2004; Powell *et al*. 2004). What makes the behavioral phenotypes in *Rab3a*$^{-/-}$ mutants so different? First, mutant lines examined in these studies have different genetic backgrounds. Hensbroek *et al*. used mice on a 129/Sv background, except for (C57BL/6JolaHsd X 129/SvImJ) F1 hybrids used in the Morris water-maze test (Hensbroek *et al*. 2003). The other three studies used hybrid 129/Sv/C57BL/6J mice with a different number of backcrossed generations, which may account for the discrepancies observed among these behavioral studies. These disparate results indicate that genetic background has a strong effect on behavioral phenotypes in *Rab3a* knockout mice. Another potential explanation for differences between the current study and those of D'Adamo *et al*. (D'Adamo *et al*. 2004), Powell *et al*. (Powell *et al*. 2004) and Hensbroek *et al*. (Hensbroek *et al*. 2003) is the age at which the mice were tested. D'Adamo and Powell *et al*. tested adults, beginning behavioral testing at or after age 12 weeks, whereas our study used younger mice (ages 6–10 weeks). Finally, as previously reported, experimental environments in different laboratories may also contribute to different behavioral observations (Crabbe *et al*. 1999).

Our studies show that the *Ebd* and loss-of-function mutations of Rab3A have subtle, if any, effects on the overall level of gene transcription. However, they have significant effects on the stability of Rab3A and rabphilin3A, as well as the binding of Rab3A to its effectors. We therefore conclude that the associated changes in behavior, including learning and memory, emotion, and the previously described anomalies in circadian rhythm and response to sleep-loss, are mediated by mutation-induced changes in the stability of and the interaction between Rab3A and its effectors. Our comparison of two *Rab3a* alleles illustrates the utility as well as challenges in linking different genetic lesions in the same gene to behavioral phenotypes.

Supplementary Material

Refer to Web version on PubMed Central for supplementary material.

Acknowledgments

We thank Yoshimi Takai for rabphilin3A construct and antibodies for rabphilin3A, Rab GDI and Rab GAP; Adam Crystal and Virginia Lee for providing HEK293 cells; Don Baldwin and Warren Ewens for advice on microarray experiments and statistical analysis; Margaret Chou and Jeff Field for advice on GTP/GDP binding experiments; Irwin Lucki for advice on the FST; Lois Maltais for help with the nomenclature and Bucan lab members for technical help and critical reading of the manuscript. This work was supported by the NIH grant (R01 MH604687) and, in part, by a grant with the Pennsylvania Department of Health.

References

Adams DJ, Dermitzakis ET, Cox T, Smith J, Davies R, Banerjee R, Bonfield J, Mullikin JC, Chung YJ, Rogers J, Bradley A. Complex haplotypes, copy number polymorphisms and coding variation in two recently divergent mouse strains. Nat Genet 2005;37:532–536. [PubMed: 15852006]

Barnes P, Good M. Impaired pavlovian cued fear conditioning in Tg2576 mice expressing a human mutant amyloid precursor protein gene. Behav Brain Res 2005;157:107–117. [PubMed: 15617777]

Becker J, Tan TJ, Trepte HH, Gallwitz D. Mutational analysis of the putative effector domain of the GTP-binding Ypt1 protein in yeast suggests specific regulation by a novel GAP activity. EMBO J 1991;10:785–792. [PubMed: 2009858]

Betz A, Thakur P, Junge HJ, Ashery U, Rhee JS, Scheuss V, Rosenmund C, Rettig J, Brose N. Functional interaction of the active zone proteins Munc13–1 and RIM1 in synaptic vesicle priming. Neuron 2001;30:183–196. [PubMed: 11343654]

Borsini F, Meli A. Is the forced swimming test a suitable model for revealing antidepressant activity? Psychopharmacology (Berl) 1988;94:147–160. [PubMed: 3127840]

Brondyk WH, McKiernan CJ, Burstein ES, Macara IG. Mutants of Rab3A analogous to oncogenic Ras mutants. Sensitivity to Rab3A-GTPase activating protein and Rab3A-guanine nucleotide releasing factor. J Biol Chem 1993;268:9410–9415. [PubMed: 8387493]

Burstein ES, Brondyk WH, Macara IG. Amino acid residues in the Ras-like GTPase Rab3A that specify sensitivity to factors that regulate the GTP/GDP cycling of Rab3A. J Biol Chem 1992;267:22715–22718. [PubMed: 1331063]

Burton JL, Burns ME, Gatti E, Augustine GJ, De Camilli P. Specific interactions of Mss4 with members of the Rab GTPase subfamily. EMBO J 1994;13:5547–5558. [PubMed: 7988552]

Castillo PE, Janz R, Sudhof TC, Tzounopoulos T, Malenka RC, Nicoll RA. Rab3A is essential for mossy fibre long-term potentiation in the hippocampus. Nature 1997;388:590–593. [PubMed: 9252190]

Charney DS, Deutch A. A functional neuroanatomy of anxiety and fear: implications for the pathophysiology and treatment of anxiety disorders. Crit Rev Neurobiol 1996;10:419–446. [PubMed: 8978989]

Crabbe JC, Wahlsten D, Dudek BC. Genetics of mouse behavior: interactions with laboratory environment. Science 1999;284:1670–1672. [PubMed: 10356397]

D'Adamo P, Menegon A, Lo Nigro C, Grasso M, Gulisano M, Tamanini F, Bienvenu T, Gedeon AK, Oostra B, Wu SK, Tandon A, Valtorta F, Balch WE, Chelly J, Toniolo D. Mutations in GDI1 are responsible for X-linked non-specific mental retardation. Nat Genet 1998;19:134–139. [PubMed: 9620768]

D'Adamo P, Welzl H, Papadimitriou S, Raffaele di Barletta M, Tiveron C, Tatangelo L, Pozzi L, Chapman PF, Knevett SG, Ramsay MF, Valtorta F, Leoni C, Menegon A, Wolfer DP, Lipp HP, Toniolo D. Deletion of the mental retardation gene Gdi1 impairs associative memory and alters social behavior in mice. Hum Mol Genet 2002;11:2567–2580. [PubMed: 12354782]

D'Adamo P, Wolfer DP, Kopp C, Tobler I, Toniolo D, Lipp HP. Mice deficient for the synaptic vesicle protein Rab3a show impaired spatial reversal learning and increased explorative activity but none of the behavioral changes shown by mice deficient for the Rab3a regulator Gdi1. Eur J Neurosci 2004;19:1895–1905. [PubMed: 15078563]

D'Hooge R, De Deyn PP. Applications of the Morris water maze in the study of learning and memory. Brain Res Brain Res Rev 2001;36:60–90. [PubMed: 11516773]

Davis M. Are different parts of the extended amygdala involved in fear versus anxiety? Biol Psychiatry 1998;44:1239–1247. [PubMed: 9861467]

Dehal P, Predki P, Olsen AS, et al. Human chromosome 19 and related regions in mouse: conservative and line-age-specific evolution. Science 2001;293:104–111. [PubMed: 11441184]

Easton A, Arbuzova J, Turek FW. The circadian Clock mutation increases exploratory activity and escape-seeking behavior. Genes Brain Behav 2003;2:11–19. [PubMed: 12882315]

Farnsworth CL, Feig LA. Dominant inhibitory mutations in the Mg(2+) -binding site of RasH prevent its activation by GTP. Mol Cell Biol 1991;11:4822–4829. [PubMed: 1922022]

Flaherty, L. Congenic strains. In: Foster, HL.; Small, JD.; Fox, JG., editors. The Mouse in Biomedical Research. Vol. Vol. 1. Academic Press; New York: 1981. p. 215-222.

Foletti DL, Scheller RH. Developmental regulation and specific brain distribution of phosphorabphilin. J Neurosci 2001;21:5461–5472. [PubMed: 11466417]

Fukui K, Sasaki T, Imazumi K, Matsuura Y, Nakanishi H, Takai Y. Isolation and characterization of a GTPase activating protein specific for the Rab3 subfamily of small G proteins. J Biol Chem 1997;272:4655–4658. [PubMed: 9030515]

Geppert M, Bolshakov VY, Siegelbaum SA, Takei K, De Camilli P, Hammer RE, Sudhof TC. The role of Rab3A in neurotransmitter release. Nature 1994;369:493–497. [PubMed: 7911226]

Geppert M, Goda Y, Stevens CF, Sudhof TC. The small GTP-binding protein Rab3A regulates a late step in synaptic vesicle fusion. Nature 1997;387:810–814. [PubMed: 9194562]

Giovedi S, Darchen F, Valtorta F, Greengard P, Benfenati F. Synapsin is a novel RAB3 effector protein on small synaaptic vesicles II. Functional effects of the Rab3A-synapsin 1 interaction. J Biol Chem 2004;279:43769–43779. [PubMed: 15265868]

Gould TJ, Feiro OR. Age-related deficits in the retention of memories for cued fear conditioning are reversed by galantamine treatment. Behav Brain Res 2005;165:160–171. [PubMed: 16154210]

Grant GR, Liu J, Stoeckert CJ Jr. A practical false discovery rate approach to identifying patterns of differential expression in microarray data. Bioinformatics 2005;21:2684–2690. [PubMed: 15797908]

Gurkan C, Lapp H, Alory C, Su AI, Hogenesch JB, Balch WE. Large-scale profiling of Rab GTPase trafficking networks: the membrome. Mol Biol Cell 2005;16:3847–3864. [PubMed: 15944222]

Hensbroek RA, Kamal A, Baars AM, Verhage M, Spruijt BM. Spatial, contextual and working memory are not affected by the absence of mossy fiber long-term potentiation and depression. Behav Brain Res 2003;138:215–223. [PubMed: 12527452]

Huang YY, Zakharenko SS, Schoch S, Kaeser PS, Janz R, Sudhof TC, Siegelbaum SA, Kandel ER. Genetic evidence for a protein-kinase-A-mediated presynaptic component in NMDA-receptor-dependent forms of longterm synaptic potentiation. Proc Natl Acad Sci USA 2005;102:9365–9370. [PubMed: 15967982]

John J, Rensland H, Schlichting I, Vetter I, Borasio GD, Goody RS, Wittinghofer A. Kinetic and structural analysis of the Mg(2+) -binding site of the guanine nucleotide-binding protein p21H-ras. J Biol Chem 1993;268:923–929. [PubMed: 8419371]

Jung V, Wei W, Ballester R, Camonis J, Mi S, Van Aelst L, Wigler M, Broek D. Two types of RAS mutants that dominantly interfere with activators of RAS. Mol Cell Biol 1994;14:3707–3718. [PubMed: 8196614]

Kapfhamer D, Valladares O, Sun Y, Nolan PM, Rux JJ, Arnold SE, Veasey SC, Bucan M. Mutations in Rab3a alter circadian period and homeostatic response to sleep loss in the mouse. Nat Genet 2002;32:290–295. [PubMed: 12244319]

Kikuchi A, Nakanishi H, Takai Y. Purification and properties of Rab3A. Methods Enzymol 1995;257:57–70. [PubMed: 8583939]

Kim JJ, Fanselow MS. Modality-specific retrograde amnesia of fear. Science 1992;256:675–677. [PubMed: 1585183]

Klinz FJ. GTP-blot analysis of small GTP-binding proteins. The C-terminus is involved in renaturation of blotted proteins. Eur J Biochem 1994;225:99–105. [PubMed: 7925476]

Koch M. The neurobiology of startle. Prog Neurobiol 1999;59:107–128. [PubMed: 10463792]

Koch M, Schnitzler HU. The acoustic startle response in rats – circuits mediating evocation, inhibition and potentiation. Behav Brain Res 1997;89:35–49. [PubMed: 9475613]

Lattal KM, Abel T. Different requirements for protein synthesis in acquisition and extinction of spatial preferences and context-evoked fear. J Neurosci 2001;21:5773–5780. [PubMed: 11466449]

Li C, Takei K, Geppert M, Daniell L, Stenius K, Chapman ER, Jahn R, De Camilli P, Sudhof TC. Synaptic targeting of rabphilin-3A, a synaptic vesicle $Ca2^{+}$/phospholipid-binding protein, depends on rab3A/3C. Neuron 1994;13:885–898. [PubMed: 7946335]

Lopez JF, Akil H, Watson SJ. Neural circuits mediating stress. Biol Psychiatry 1999;46:1461–1471. [PubMed: 10599476]

Lucki I, Dalvi A, Mayorga AJ. Sensitivity to the effects of pharmacologically selective antidepressants in different strains of mice. Psychopharmacology (Berl) 2001;155:315–322. [PubMed: 11432695]

Luo HR, Saiardi A, Nagata E, Ye K, Yu H, Jung TS, Luo X, Jain S, Sawa A, Snyder SH. GRAB: a physiologic guanine nucleotide exchange factor for Rab3A, which interacts with inositol hexakisphosphate kinase. Neuron 2001;31:439–451. [PubMed: 11516400]

Matsui Y, Kikuchi A, Araki S, Hata Y, Kondo J, Teranishi Y, Takai Y. Molecular cloning and characterization of a novel type of regulatory protein (GDI) for smg p25A, a ras p21-like GTP-binding protein. Mol Cell Biol 1990;10:4116–4122. [PubMed: 2115118]

Matus-Amat P, Higgins EA, Barrientos RM, Rudy JW. The role of the dorsal hippocampus in the acquisition and retrieval of context memory representations. J Neurosci 2004;24:2431–2439. [PubMed: 15014118]

Nagano F, Sasaki T, Fukui K, Asakura T, Imazumi K, Takai Y. Molecular cloning and characterization of the noncatalytic subunit of the Rab3 subfamily-specific GTPase-activating protein. J Biol Chem 1998;273:24781–24785. [PubMed: 9733780]

Nagano F, Kawabe H, Nakanishi H, Shinohara M, Deguchi-Tawarada M, Takeuchi M, Sasaki T, Takai Y. Rabconnectin-3, a novel protein that binds both GDP/GTP exchange protein and GTPase-activating protein for Rab3 small G protein family. J Biol Chem 2002;277:9629–9632. [PubMed: 11809763]

Ostermeier C, Brunger AT. Structural basis of Rab effector specificity: crystal structure of the small G protein Rab3A complexed with the effector domain of rabphilin-3A. Cell 1999;96:363–374. [PubMed: 10025402]

Owen EH, Christensen SC, Paylor R, Wehner JM. Identification of quantitative trait loci involved in contextual and auditory-cued fear conditioning in BXD recombinant inbred strains. Behav Neurosci 1997a;111:292–300. [PubMed: 9106670]

Owen EH, Logue SF, Rasmussen DL, Wehner JM. Assessment of learning by the Morris water task and fear conditioning in inbred mouse strains and F1 hybrids: implications of genetic background for single gene mutations and quantitative trait loci analyses. Neuroscience 1997b;80:1087–1099. [PubMed: 9284062]

Pezze MA, Feldon J. Mesolimbic dopaminergic pathways in fear conditioning. Prog Neurobiol 2004;74:301–320. [PubMed: 15582224]

Phillips RG, LeDoux JE. Differential contribution of amygdala and hippocampus to cued and contextual fear conditioning. Behav Neurosci 1992;106:274–285. [PubMed: 1590953]

Powell CM, Schoch S, Monteggia L, Barrot M, Matos MF, Feldmann N, Sudhof TC, Nestler EJ. The presynaptic active zone protein RIM1alpha is critical for normal learning and memory. Neuron 2004;42:143–153. [PubMed: 15066271]

Rak A, Pylypenko O, Durek T, Watzke A, Kushnir S, Brunsveld L, Waldmann H, Goody RS, Alexandrov K. Structure of Rab GDP-dissociation inhibitor in complex with prenylated YPT1 GTPase. Science 2003;302:646–650. [PubMed: 14576435]

Rosahl TW, Spillane D, Missler M, Herz J, Selig DK, Wolff JR, Hammer RE, Malenka RC, Sudhof TC. Essential functions of synapsins I and II in synaptic vesicle regulation. Nature 1995;375:488–493. [PubMed: 7777057]

Sakai T, Tamura T, Kitamoto T, Kidokoro Y. A clock gene, period, plays a key role in long-term memory formation in Drosophila. Proc Natl Acad Sci USA 2004;101:16058–16063. [PubMed: 15522971]

Sasaki T, Kikuchi A, Araki S, Hata Y, Isomura M, Kuroda S, Takai Y. Purification and characterization from bovine brain cytosol of a protein that inhibits the dissociation of GDP from and the subsequent binding of GTP to smg p25A, a ras p21-like GTP-binding protein. J Biol Chem 1990;265:2333–2337. [PubMed: 2105320]

Schluter OM, Schnell E, Verhage M, Tzonopoulos T, Nicoll RA, Janz R, Malenka RC, Geppert M, Sudhof TC. Rabphilin knock-out mice reveal that rabphilin is not required for rab3 function in regulating neurotransmitter release. J Neurosci 1999;19:5834–5846. [PubMed: 10407024]

Schluter OM, Khvotchev M, Jahn R, Sudhof TC. Localization versus function of Rab3 proteins. Evidence for a common regulatory role in controlling fusion. J Biol Chem 2002;277:40919–40929. [PubMed: 12167638]

Schluter OM, Schmitz F, Jahn R, Rosenmund C, Sudhof TC. A complete genetic analysis of neuronal Rab3 function. J Neurosci 2004;24:6629–6637. [PubMed: 15269275]

Schoch S, Castillo PE, Jo T, Mukherjee K, Geppert M, Wang Y, Schmitz F, Malenka RC, Sudhof TC. RIM1alpha forms a protein scaffold for regulating neurotransmitter release at the active zone. Nature 2002;415:321–326. [PubMed: 11797009]

Shirataki H, Kaibuchi K, Yamaguchi T, Wada K, Horiuchi H, Takai Y. A possible target protein for smg-25A/rab3A small GTP-binding protein. J Biol Chem 1992;267:10946–10949. [PubMed: 1597436]

Shirataki H, Kaibuchi K, Sakoda T, Kishida S, Yamaguchi T, Wada K, Miyazaki M, Takai Y. Rabphilin-3A, a putative target protein for smg p25A/rab3A p25 small GTP-binding protein related to synaptotagmin. Mol Cell Biol 1993;13:2061–2068. [PubMed: 8384302]

Silver, LM. Mouse Genetics: Concepts and Applications. Oxford University Press; New York: 1995.

Staunton J, Ganetzky B, Nonet ML. Rabphilin potentiates soluble N-ethylmaleimide sensitive factor attachment protein receptor function independently of rab3. J Neurosci 2001;21:9255–9264. [PubMed: 11717359]

Stettler O, Moya KL, Zahraoui A, Tavitian B. Developmental changes in the localization of the synaptic vesicle protein rab3A in rat brain. Neuroscience 1994;62:587–600. [PubMed: 7830899]

Sudhof TC. The synaptic vesicle cycle. Annu Rev Neurosci 2004;27:509–547. [PubMed: 15217342]

Swerdlow NR, Geyer MA, Braff DL. Neural circuit regulation of prepulse inhibition of startle in the rat: current knowledge and future challenges. Psychopharmacology (Berl) 2001;156:194–215. [PubMed: 11549223]

Takai Y, Sasaki T, Shirataki H, Nakanishi H. Rab3A small GTP-binding protein in Ca(2)-dependent exocytosis. Genes Cells 1996;1:615–632. [PubMed: 9078389]

Takai Y, Sasaki T, Matozaki T. Small GTP-binding proteins. Physiol Rev 2001;81:153–208. [PubMed: 11152757]

Tarantino LM, Gould TJ, Druhan JP, Bucan M. Behavior and mutagenesis screens: the importance of baseline analysis of inbred strains. Mamm Genome 2000;11:555–564. [PubMed: 10886023]

Ullrich O, Stenmark H, Alexandrov K, Huber LA, Kaibuchi K, Sasaki T, Takai Y, Zerial M. Rab GDP dissociation inhibitor as a general regulator for the membrane association of rab proteins. J Biol Chem 1993;268:18143–18150. [PubMed: 8349690]

Wada M, Nakanishi H, Satoh A, Hirano H, Obaishi H, Matsuura Y, Takai Y. Isolation and characterization of a GDP/GTP exchange protein specific for the Rab3 subfamily small G proteins. J Biol Chem 1997;272:3875–3878. [PubMed: 9020086]

Wagner P, Molenaar CM, Rauh AJ, Brokel R, Schmitt HD, Gallwitz D. Biochemical properties of the rasrelated YPT protein in yeast: a mutational analysis. EMBO J 1987;6:2373–2379. [PubMed: 3311726]

Wang Y, Sudhof TC. Genomic definition of RIM proteins: evolutionary amplification of a family of synaptic regulatory proteins (small star, filled). Genomics 2003;81:126–137. [PubMed: 12620390]

Wang Y, Okamoto M, Schmitz F, Hofmann K, Sudhof TC. Rim is a putative Rab3 effector in regulating synaptic-vesicle fusion. Nature 1997;388:593–598. [PubMed: 9252191]

Wang Y, Sugita S, Sudhof TC. The RIM/NIM family of neuronal C2 domain proteins. Interactions with Rab3 and a new class of Src homology 3 domain proteins. J Biol Chem 2000;275:20033–20044. [PubMed: 10748113]

Wieland S, Lucki I. Antidepressant-like activity of 5-HT1A agonists measured with the forced swim test. Psychopharmacology (Berl) 1990;101:497–504. [PubMed: 1975107]

Zerial M, McBride H. Rab proteins as membrane organizers. Nat Rev Mol Cell Biol 2001;2:107–117. [PubMed: 11252952]

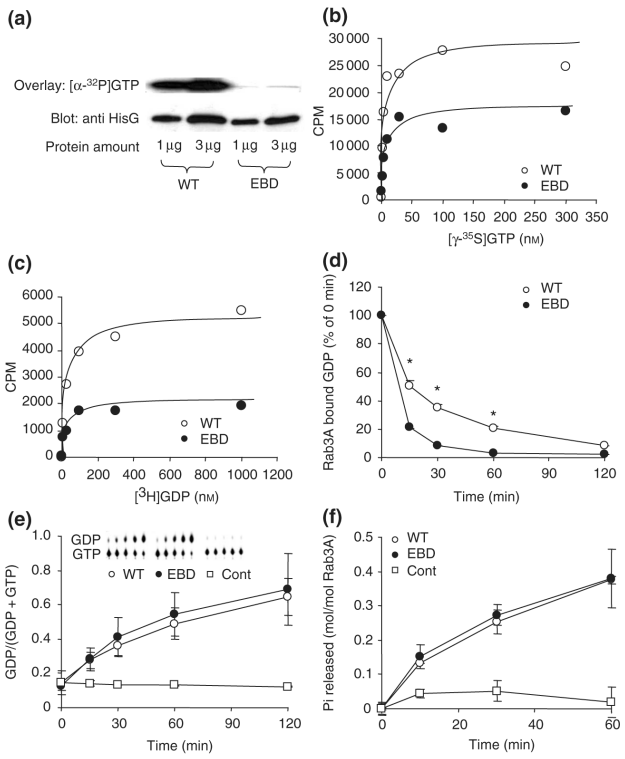

Figure 1. Biochemical analysis of wild-type (WT) and *earlybird* mutant (EBD) ras-associated binding (Rab) protein 3A

(a) [α-^{32}P]guanosine triphosphate (GTP) overlay assay was performed by blotting wild-type and mutant proteins to PVDF membranes, which were either incubated with [α-^{32}P]GTP to examine GTP binding (upper panel) or subjected to immunoblotting to visualize protein content (lower panel). (b) A saturation GTP binding assay was performed by incubating Rab3A proteins with various concentrations of [γ-^{35}S]GTP. Figure shown is a representative result of three independent experiments. (c) A [^{3}H]GDP binding assay was performed in a similar manner as [γ-^{35}S]GTP binding assay described in (b). (d) The GDP dissociation assay was started by adding an extra amount of GTP and GDP after loading proteins with [^{3}H]GDP. The radioactivity was normalized to time zero and plotted as a function of time. *$P < 0.01$, student's *t*-test. (e) GTPase activity assessed using thin layer chromatography (TLC) method. The GDP amount generated was plotted against time of incubation. The control experiments contain no protein. The intersect shows a representative TLC image. Data shown are means ± SD of three independent experiments. (f) GTPase activity assessed using the charcoal method. The amount of Pi released was plotted against time of incubation. No protein was included in the control experiments. Data represent means ± SD of two independent experiments in duplicates.

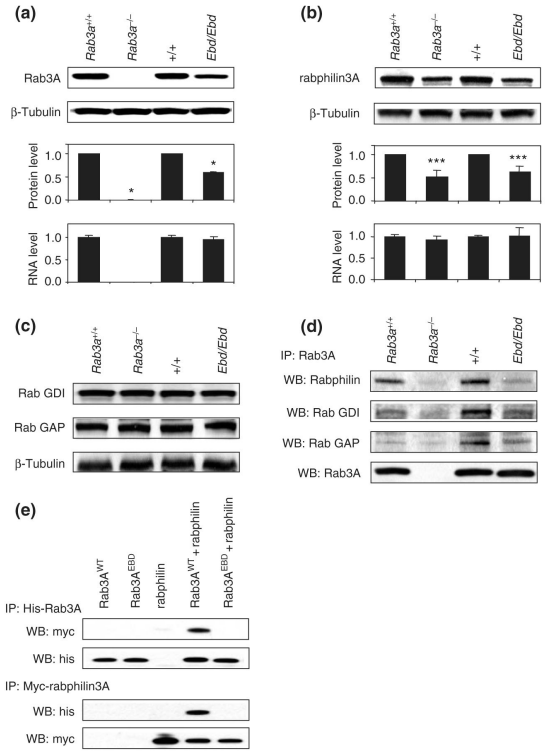

Figure 2. Protein stability of ras-associated binding (Rab) protein 3A and its effectors and their interactions in mutant mice

(a) Rab3A protein levels were examined by immunoblotting with anti-Rab3A in homogenates from the hippocampus of *earlybird (Ebd)* and *Rab3a* null mice. The upper two panels show the representative Western blots for indicated wild-type and mutant strains of mice. The protein levels were quantified using ImageJ and normalized to β-tubulin. The mRNA levels of Rab3A measured by real-time quantitative polymerase chain reaction. Data are means ± SD. $*P < 0.001$, student's *t*-test. (b) Rabphilin3A protein levels (upper and middle panels) and mRNA levels (lower) in the hippocampus of *Ebd* and *Rab3a*-null mice were examined similarly as described in (a). (c) Protein levels of Rab GDI and Rab GAP in the cortex of *Ebd* and *Rab3a*-null mice were examined by Western blot using anti-Rab GDI1 and anti-Rab GAP p130 antibodies. Beta-tubulin was also examined as a control for sample input. (d) Co-immunoprecipitation in the cortex homogenates. Rab3A was immunoprecipitated with anti-Rab3A antibodies, and Rab3A-bound rabphilin3A, Rab GDI and Rab GAP were detected using respective antibodies in Western blot. Anti-Rab3A antibodies were used to examine the sample input (lower panel). (e) Co-immunoprecipitation in the lysates of HEK 293 cells co-transfected with His-tagged Rab3A and Myc-tagged rabphilin3A.

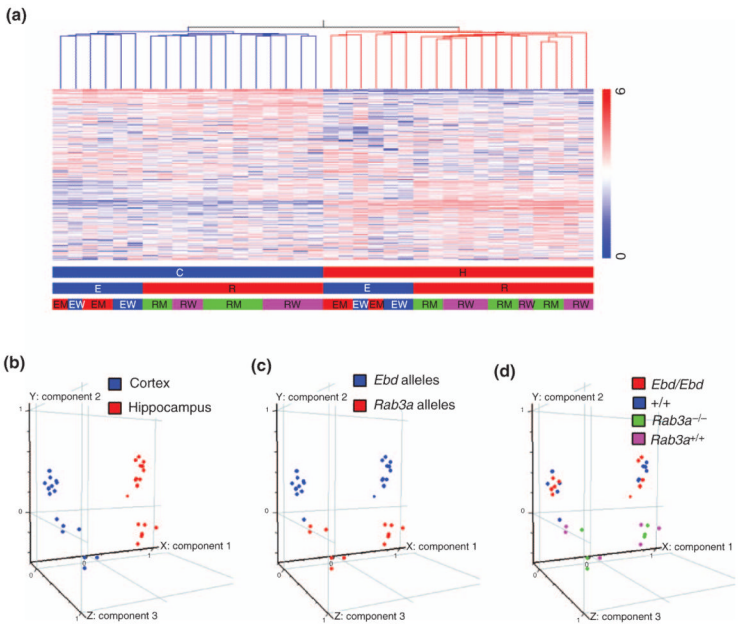

Figure 3. Global profiling of the 36 microarray samples from cortex and hippocampus of *earlybird (Ebd)* and *Rab3a*-null mutants and their wild-type littermates

(a) Hierarchical clustering of the 20975 genes across 36 samples. Pearson correlation was used to construct the gene tree and the condition tree (only the condition tree is shown). Normalized expression values are displayed according to the vertical color bar. The horizontal bars beneath indicate the sample information: C, cortex; H, hippocampus; E, *Ebd* line; R, *Rab3a* null line; EM, *Ebd/Ebd*;EW, +/+ (wild-type controls of *Ebd/Ebd*); RM, $Rab3a^{-/-}$; RW, $Rab3a^{+/+}$. (b–d) Principle Component Analysis on these 36 samples. (b) Different brain regions are distributed along the first component that contributed 24.09% to the overall variance in the gene expression among these 36 samples. (c) Genetic backgrounds are distributed along the second component that had a contribution of 10.08%. (d) The four different genotypes do not show clear distribution pattern, indicating that *Ebd* or *Rab3a*-null mutation had subtle effect on gene expression.

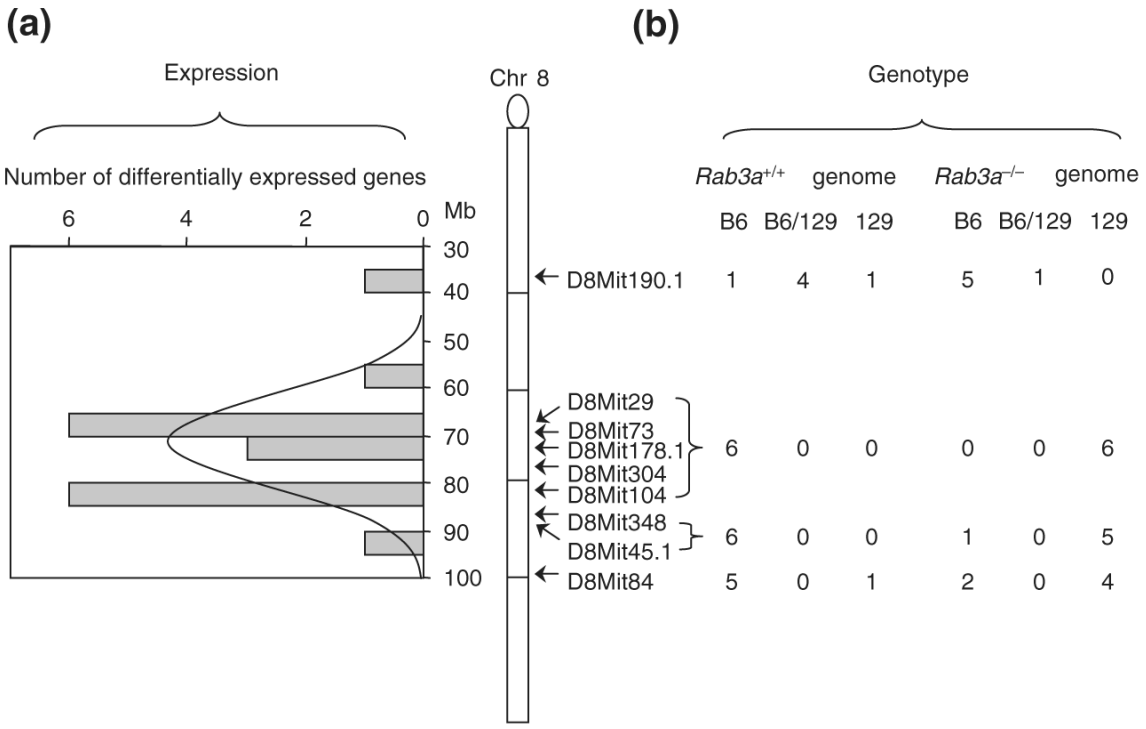

Figure 4. Differentially expressed genes in *Rab3a*$^{-/-}$ mice map to a congenic chromosomal region derived from the 129 strain

(a) Distribution of differentially expressed genes on chromosome 8. The map position of the differential genes in the cortex and the hippocampus of *Rab3a*$^{-/-}$ mice showed a distribution similar to normal distribution as indicated by the curve. The distribution centered at the *Rab3a* locus. (b) Genotypes of the *Rab3a*$^{+/+}$ and *Rab3a*$^{-/-}$ mice at 9 loci around *Rab3a* gene. The positions of the markers are indicated by the arrows along chromosome 8. To the right of the markers are numbers of the animals that were homozygous for C57BL/6J (B6), homozygous for 129/Sv (129) or heterozygous (B6/129) at markers indicated.

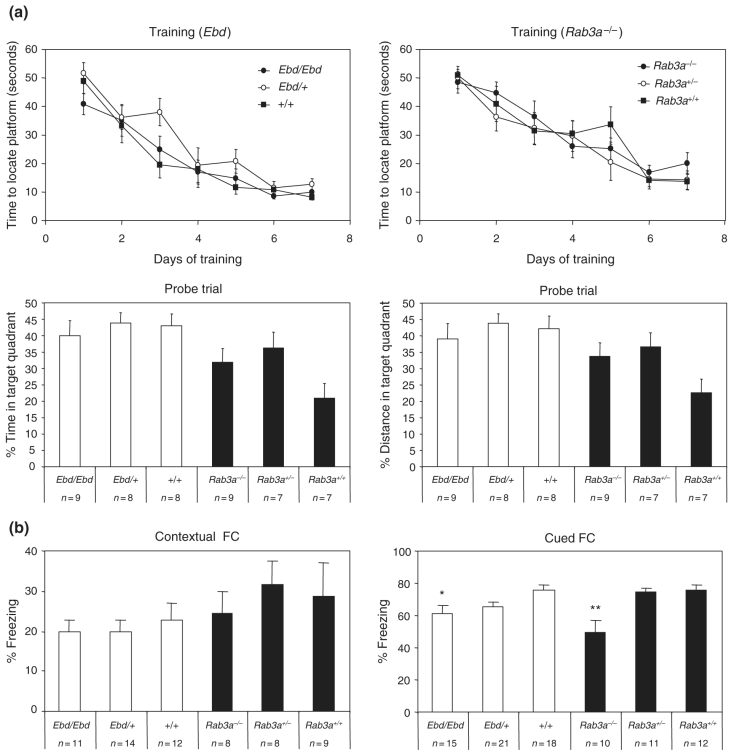

Figure 5. Learning and memory deficits in *earlybird* (*Ebd*) and *Rab3a*$^{-/-}$ mice

(a) Spatial learning and memory in the hidden platform version of the Morris water-maze test. The upper panels show the performance of *Ebd* (left) and *Rab3a*$^{-/-}$ (right) mice in the training trials. The lower panels show the performance in the probe trial. (b) Fear conditioning (FC). Hippocampal-dependent learning was examined by measuring freezing behavior upon presentation of the chamber (contextual FC), and amygdala-dependent learning was assessed by presentation of the white noise stimulus (cued FC). Data shown are means ± SEM. *$P < 0.05$; **$P < 0.01$, Tukey HSD test after one-way analysis of variance.

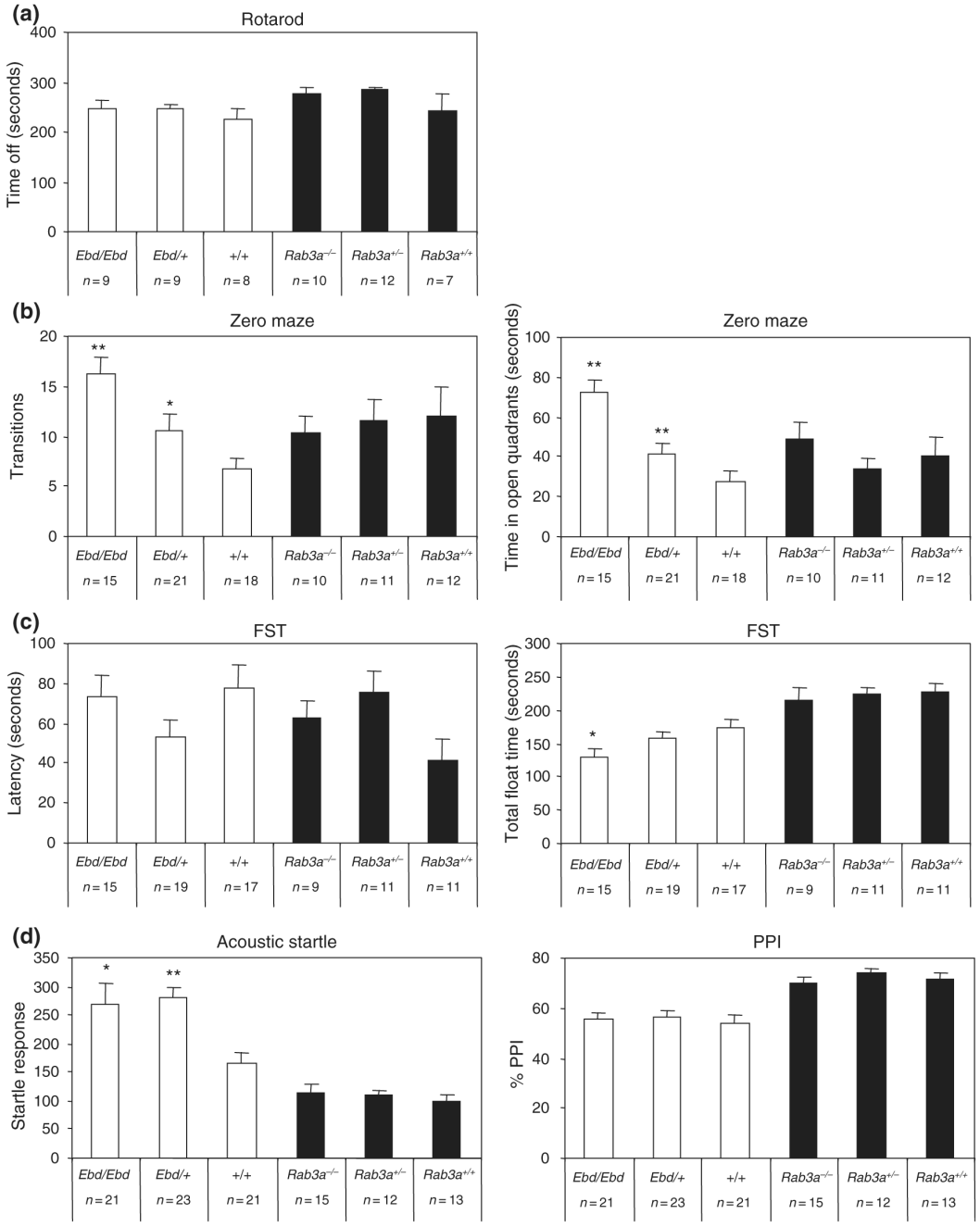

Figure 6. *Earlybird* (*Ebd*) mice but not *Rab3a*$^{-/-}$ mice showed abnormal emotional status

(a) Both the *Ebd* mice and the *Rab3a*-null mice have normal motor co-ordination on the accelerated rotarod. (b) *Ebd* mice displayed reduced anxiety-like behavior in the zero maze test. (c) *Ebd* mice showed reduced immobility in the Forced swim test. (d) *Ebd* mice had increased startle response compared to wild-type controls but showed normal prepulse Inhibition. Data shown are means ± SEM. **P* < 0.05; ***P* < 0.01, Tukey HSD test after one-way analysis of variance.

Table 1

Differentially expressed genes in the *Earlybird* and *Rab3a*$^{-/-}$ mice

Gene Name	Affy ID	FC[#]	Location[##]	Description
cem/cew[*]				
Morc2a	1456398_at	1.62	11:3610702	Microrchidia 2A
Casp8	1424552_at	1.53	1:59046582	Caspase 8
Dad1	1454860_x_at	0.62	14:49105685	Defender against cell death 1
hem/hew[**]				
Ptgds	1423860_at	0.53	2:25474022	Prostaglandin D2 synthase (brain)
Ttr	1455913_x_at	0.39	18:21036130	Transthyretin
crm/crw[***]				
C030044C12Rik	1429097_at	0.66	8:82332807	RIKEN cDNA C030044C12 gene
Atp11c	1437600_at	0.66	X:55703999	Atpase, class VI, type 11C
5330410G16Rik	1452825_at	0.63	8:68939012	RIKEN cDNA 5330410G16 gene
Chd9	1459450_at	0.63	8:89421405	Chromodomain helicase DNA binding protein 9
Rasd2	1427344_s_at	0.62	8:74420202	RASD family, member 2
Zfp617	1449546_a_at	0.62	8:70422797	Similar to hypothetical protein FLJ38281
6430500C12Rik	1453402_at	0.57	8:38069818	AV338754 RIKEN full-length enriched, cDNA clone 6430500C12
Slc5a5	1436239_at	0.55	8:69338006	Solute carrier family 5 (sodium iodide symporter), member 5
Trmt1	1436494_x_at	0.51	8:83273987	TRM1 tRNA methyltransferase 1 homolog (S. cerevisiae)
	1447892_at	0.43	18:23434305	Similar to glyceraldehyde-3-phosphate dehydrogenase
	1420287_at	0.39	8:83678096	Transcribed locus
C030036D22Rik	1443744_at	0.36	18:72562266	RIKEN cDNA C030036D22 gene
Large	1460113_at	0.35	8:71338357	Like-glycosyltransferase
Usp38	1428592_s_at	0.29	8:79520109	Ubiquitin specific protease 38
	1444260_at	0.2	8:68465175	Weakly similar to XP_227873.2 similar to RIKEN cDNA 9330196J05
Prdx2	1430979_a_at	0.14	8:83555736	Peroxiredoxin 2
Rab3a	1422589_at	0.01	8:69208775	RAB3A, member RAS oncogene family
hrm/hrw[****]				
Lpl	1431056_a_at	2.4	8:67335311	Lipoprotein lipase
Xrn1	1442141_at	1.72	9:95600697	5′-3′ exoribonuclease 1

Gene Name	Affy ID	FC[#]	Location[##]	Description
Mfap3l	1428804_at	1.63	8:59024530	Microfibrillar-associated protein 3-like
Slc13a4	1433734_at	1.54	6:35199160	Solute carrier family 13 (sodium/sulfate symporters), member 4
Large	1443212_at	0.65	8:71338357	Like-glycosyltransferase
C030044C12Rik	1429097_at	0.63	8:82332807	RIKEN cDNA C030044C12 gene
Pgpep1	1418329_at	0.62	8:69104250	Pyroglutamyl-peptidase I
Zfp330	1451216_at	0.61	8:81326159	Zinc finger protein 330
5330410G16Rik	1452825_at	0.58	8:68939012	RIKEN cDNA 5330410G16 gene
Slc5a5	1436239_at	0.55	8:69338006	Solute carrier family 5 (sodium iodide symporter), member 5
Trmt1	1436494_x_at	0.54	8:83273987	TRM1 tRNA methyltransferase 1 homolog (S. cerevisiae)
Zfp617	1449546_a_at	0.48	8:70422797	Similar to hypothetical protein FLJ38281
Usp38	1428592_s_at	0.39	8:79520109	Ubiquitin specific protease 38
Prdx2	1430979_a_at	0.11	8:83555736	Peroxiredoxin 2
Rab3a	1422589_at	0.02	r8:69208775	RAB3A, member RAS oncogene family

[#]Fold Change.

[##]start site for genes or probesets are from NCBI m34 mouse assembly.

*comparison between the cortex of *Ebd/Ebd* mice (cem) and their wild-type littermates (cew).

**comparison between the hippocampus of *Ebd/Ebd* mice (hem) and their wild-type littermates (hew).

***comparison between the cortex of $Rab3a^{-/-}$ (crm) and $Rab3a^{+/+}$ mice (crw).

****comparison between the hippocampus of $Rab3a^{-/-}$ (hrm) and $Rab3a^{+/+}$ mice (hrw).